Local trade-offs shape flower size evolution across *Arabidopsis thaliana* distribution.

Kevin Sartori[1*], Clàudia F. Mestre[1], Md Jonaid Hossain[1], Aurélien Estarague[2], Elza Gaignon[2], Pierre Moulin[2], Jesse R. Lasky[3], Denis Vile[4], Francois Vasseur[2,4], Cyrille Violle[2] and Adrien Sicard[1*].

[1] Department of Plant Biology, Swedish University of Agricultural, Sciences and Linnean Center for Plant Biology, Uppsala, Sweden.

[2] CEFE, Univ Montpellier, CNRS, EPHE, IRD, Montpellier, France

[3] Department of Biology and PAC Herbarium, Pennsylvania State University, University Park, PA, USA

[4] Laboratoire d'Ecophysiologie des Plantes sous Stress Environnementaux (LEPSE), INRA, Montpellier SupAgro, UMR, Montpellier, France.

* Corresponding authors: kevin.sartori@slu.se ; adrien.sicard@slu.se

Abstract

The evolution of flowers, largely driven by mutualistic interactions with animal pollinators, resulted in a vast diversity of shape and size that was believed to have spurred the intense evolutionary radiation in angiosperms. In this study, we investigate the geographic variation in reproductive organ growth in the self-fertilizing species *Arabidopsis thaliana*, where the absence of pollinator requirement for reproduction is expected to promote the reduction of flower organ sizes to optimize resource allocation. We find large variation in flower size associated with a polygenic architecture in which derived alleles increase or decrease flower size, and exhibit signs of positive selection. The variation in the direction of flower size evolution is associated with a clear biogeographic pattern emerging from environmentally driven fluctuations in the flower size-seed production relationship. Stronger purifying selection at climatic range margins favors smaller flowers, while relaxed environmental constraints in more suitable habitats allow for the fixation of potentially adaptive large-flower mutations. Such a geographical pattern extends to other life history traits, demonstrating how environmental heterogeneity, in interaction with resource allocation constraints, shapes evolutionary trajectories and phenotypic diversity.

Introduction

Natural selection maximizes reproductive success by optimizing resource allocation among growth, survival, and reproduction, with trade-offs between traits shaping phenotypic evolution under resource constraints (Parker & Smith, 1990) (Kozłowski, 1992; Adler et al., 2013). While environmental heterogeneity affects resource acquisition and selection (Troth et al., 2018), its role in shaping molecular evolution and phenotypic diversification across environmental gradients and species ranges remains poorly understood.

Flowers construction and maintenance costs tend to increase with the likelihood of fertilization, imposing major trade-offs in plants (Roddy et al., 2020). The resource allocation constraints on flower evolution are manifested, for instance, by the existence of a trade-off between flower number and size in many species (Caruso, 2006; Worley & Barrett, 2000). Under such constraints, the wide radiation of flowering plants is believed to result from the evolution of specialized plant-pollinator interactions, leading to an immense diversification in flower morphology and physiology (Crane et al., 1994; Friis et al., 1994, 1999, 2006; Galen, 1999). The importance of resource partitioning in driving flower and plant evolution is best suggested by pervasive trends across plant phylogeny, such as the repeated emergence of self-fertilizing lineages from animal-pollinated outcrosser ancestors (Stebbins, 1957). When a species transitions to self-fertilization, the resources initially invested to construct large and attractive flowers can be reallocated to other traits to maximize fitness. This hypothesis has been proposed to explain the general decline of flower attractiveness, known as the selfing syndrome, often observed after the emergence of selfing lineages (Sicard et al., 2011). Because pollinator-mediated selection in such lineages is limited, they constitute ideal natural experiments to investigate the interplay between latent trade-offs, environment heterogeneity and micro-evolutionary processes shaping reproductive organ diversification. Evolutionary theories often cite resource allocation constraints as the primary explanation for the selfing syndrome, frequently overlooking other potential evolutionary drivers.

Under the hypothesis that flower organ growth imposes significant construction costs, constraints in resource allocation are expected to alter the trajectory of flower evolution after the transition to self-fertilization. Mutations that reduce expenses in flower organ growth, especially those involved in pollinator attraction (e.g., petals), are likely to be selected, as they allow for saving resources that are reallocated to various fitness components such as ovule or flower numbers (Charlesworth & Charlesworth, 1981). Smaller reproductive organs should thus be associated with higher fitness in selfing species, resulting in a selective trade-off between flower size and, for instance, seed production. Consequently, these mutations are expected to rapidly increase in frequency across populations, leaving characteristic genomic imprints of directional selection (Stephan, 2019). Independent selfing lineages within such species should, therefore, converge towards small-sized flowers, consequently reducing

intraspecific variance. Nevertheless, environmental heterogeneity creates variation in habitat suitability for a species by modulating resource availability and/or imposing developmental and phenological constraints (e.g., harsh periods avoidance) and is, therefore, likely to influence the intensity of selection pressures on resource allocation strategies (Fu et al., 2010; MacTavish & Anderson, 2020; Tuller et al., 2018). Such heterogeneity could also drive diversification in flower size if others ecological pressures promoting large flower phenotypes, for instance to increase outcrossing rates or to attract protective insects (Hoffmann et al., 2003; Poecke, 2007) counterbalance the resource allocation benefits of smaller petals.

Alternatively, the evolutionary pressures to maintain large flowers could simply be relaxed if the loss of pollinator-attractive attributes does not confer fitness benefits through resource reallocation. Consequently, flower size would be mostly influenced by genetic drift, resulting in less predictable changes, including increasing phenotypic variance and leaving no distinct signature of directional selection at the underlying loci (Woźniak & Sicard, 2018). The lack of selective pressure to maintain large flowers, combined with reduced effective recombination due to increased homozygosity in selfing lineages, could increase the probability of fixation of non-synonymous mutations through genetic drift, potentially impairing genes that promote flower growth (Barrett et al., 2014).

Gene pleiotropy or linked selection could also influence flower size evolution (Chebib & Guillaume, 2017; Slotte, 2014), especially in selfing lineages where low level of effective recombination further increases linkage disequilibrium. If genes controlling flower size also influence the size of other organs or other phenotypes, a pattern that could be expected based on the known pleiotropic effects of most plant growth regulators (Johnson & Lenhard, 2011), then selection on other traits, such as leaf size, could lead to correlated changes with floral traits. If pleiotropy is predominant, it could even result in an isometric correlation between phenotypes (with a slope of 1). However, as the influence of pleiotropy declines, correlated changes may become more allometric (deviating from a slope equal to 1), reflecting the effects of shared evolutionary constraints instead (Huxley et al., 1993). Linked selection can have similar effects, locally reducing or promoting genetic diversity at loci neighbouring sites under selection, with the extent of its influence depending on the recombination rate (Slotte, 2014). Although linked selection can cause changes in phenotypes other than the trait under selection, creating genetic linkages between traits, it may not always result in phenotypic correlations at the species level. This is because the direction of changes in linked phenotypes can depend on local genetic diversity. Given the diversity of processes that can influence flower size evolution, it is expected that a large number of mutations would underlie flower size variation, consistent with the polygenic nature of flower size evolution associated with the transition to selfing (Sicard et al., 2011; Sicard & Lenhard, 2011; Woźniak et al., 2020). However, the relative contributions of various processes to flower size evolution remain poorly understood.

The plant model *Arabidopsis thaliana* provides a robust system for studying the biogeographical patterns of molecular evolution driving flower size evolution. Selfing in this species has recently emerged, preceding a rapid colonization during which it spread into different lineages (Bechsgaard et al., 2006; Shimizu & Tsuchimatsu, 2015; Tang et al., 2007). Consequently, diverse mutations affecting flower size likely became fixed across different lineages, potentially leading to variations across populations (Tsuchimatsu et al., 2020). Furthermore, pollinators may have limited influence on flower evolution in this species. Leveraging the extensive genomic and phenotypic resources available for *A. thaliana*, we aimed to explore the genetic and ecological factors influencing the evolution of flower size following the emergence of selfing. Our findings support the idea that phenotypic evolution trajectories vary across the species' range distribution due to differential selection pressures shaped by environmental gradients.

Results and discussion

Flower size is highly variable within A. thaliana

The selfing syndrome theory predict that flower size and its variance must decrease in self-fertilizing species such as *Arabidopsis thaliana* due to the existence of resource allocation trade-offs. Alternatively, genetic and phenotypic variation may persist if genetic drift is the main force involved (Buysse et al., 2024) or if environmental drivers persist (MacTavish & Anderson, 2020). To test these hypotheses, we investigated species-wide variation in investment in floral organs and compared it to that of vegetative organs. To this end, we measured the length, width and area of flower organs and leaves of 407 *A. thaliana* accessions chosen to encompass the species-wide genetic and geographic diversity (**Fig. S1, Table S1**). All traits exhibited significant variation within our dataset, roughly following a normal distribution (**Fig. S2**). The variation in flower organ size emerged as a significant factor contributing to the phenotypic diversity among the sampled accessions (**Fig. 1a**). A principal component analysis applied to leaf and flower organ traits revealed that the largest part of the variance (43.2% - PC1) is explained by variation in flower organ size, with correlation coefficients above 0.5 for all flower organ traits. Meanwhile, the second PC (21.6% of the variance) summarized only leaf size traits ($r > 0.5$). Other reproductive traits were less variable across accessions. Ovule number exhibited the strongest correlation with the fourth principal component (PC), explaining less than 8% of the variance. Among floral organs, petal area was the most variable, displaying a coefficient of variation similar to leaf area, with over three-fold changes between extreme values (**Table S2**). Based on these observations, we hypothesized that flower size variability within this species might be attributed to the ongoing evolution of selfing syndrome (i.e., the fixation of mutations that reduce flower size in some but not all lineages of the species) or due to heterogeneous selection pressures across populations.

Independent, low-pleiotropy mutations largely account for the variation in flower organ sizes.

We investigated whether indirect effects, such as linked selection (Smith & Haigh, 1974) or a common genetic basis (pleiotropy) shared with other traits under selection, drive flower size evolution in *A. thaliana*. To this end, we first tested whether flower organ size covaries with other traits among genotypes (**Table S2**). Stamen, petal and sepal size components were significantly positively correlated to each other (r ranging from 0.28 to 0.93) but uncorrelated with ovule number and leaf size traits (although leaf length weakly correlated with petal width, with r=-0.15) (**Fig. 1b**). The long stamen length to petal length relationship was strictly isometric (slope = 1, P-value > 0.01) suggesting that shared genetic bases are involved in their development, while other pairwise relationships were allometric, increasing by less than one unit for one unit increase in stamen length or petal size (slope < 1, P-value < 0.001). Nevertheless, all flower organs were significantly positively correlated with flowering time (correlation coefficient r ranging from 0.14 to 0.42), which was also significantly negatively correlated with ovule number (r = -0.33). We further tested for correlation with phenotypes available in the literature. None of our flower organ size traits significantly correlated with any of the 107 phenotypes from (Atwell et al. 2010), while flowering time correlated significantly with life cycle and plant biomass-related traits (**Table S2**). Specific leaf area (SLA), leaf nitrogen content (LNC), and plant biomass from (Przybylska et al. 2023) significantly correlated with several flower size traits (r ranging from -0.35 to 0.4), and most traits correlated with flowering time (r ranging from -0.67 to 0.70). Significant phenotypic correlation can arise because of independent evolution caused by a coordinated response to environmental pressure or due to a shared genetic basis (pleiotropy). We, thus, specifically investigated the role of genetic correlations in the observed trait covariation.

For this purpose, we performed a multivariate Genome-Wide Association study (mGWAS) for significantly correlated trait pairs. This method partitions the genetic variance into trait-specific genetic variances and the part of genetic variance explaining both traits, i.e. the genetic correlation (r_g). This allows to determine to which extent two traits are influenced by shared genetic variants (Zhou & Stephens, 2014) (**Table S3**). We detected no significant genetic correlation between flower and leaf traits, suggesting that the evolution of these organs' size has independent genetic bases. Ovule number presented a significant genetic correlation (r_g ~0.4; P-value<0.01) with SLA and LNC, two traits used as a proxy for plant resource acquisition ability in functional ecology (Pérez-Harguindeguy et al., 2013). Petal and sepal areas presented low, yet statistically significant genetic correlation (r_g ~0.3; P-value<0.01) with LNC and whole plant dry mass. This further suggests that, to a small extent, the genetic architecture of plant resources acquisition affect both vegetative carbon economy and reproductive organ growth, which supports the hypothesis that resource allocation constraints flower size evolution. Overall, flower organ size variation is poorly correlated with most reported traits and is largely associated with independent genetic variation suggesting that pleiotropy and linked selection have little influence on petal size evolution in this species.

We further performed univariate GWAS to detect individual trait genetic bases (**Fig. 1c**). Despite a high phenotypic variance explained (PVE; the SNP-based heritability) measured for all flower organ traits ($0.55 < PVE < 0.85$), only three association peaks exceeded the Bonferroni threshold for sepal, petal and stamen traits, suggesting that most of the traits investigated have a polygenic basis (**Fig. 1c**). While two of these peaks were specific to individual organs (**Fig. 1c** right and left panels), the third peak revealed a shared genetic association between petal and sepal traits (**Fig. 1c** middle panel). To account for the polygenic architecture of the traits, we relaxed the detection threshold to $P < 5.2*10^{-5}$, based on the significance of well-established genetic associations (see Methods). We listed all genes putatively genetically linked to the candidate SNPs, including mutations within coding regions or cis-regulatory sequences (defined as the 5Kbp surrounding the genes). After filtering out linked SNPs, we identified 61, 105, 87, 59 and 38 SNPs, and 144, 191, 194, 126 and 117 genes associated with leaf, petal, sepal and stamen size traits and ovule number, respectively (**Fig. 1d, Table S4**). We next used TAIR gene ontology terms (Huala et al., 2001) to annotate gene functions and further refer to as *a priori* candidates for genes involved in growth and development. Among the gene sets, we identified well-known growth regulators, including *JAGGED*, *GROWTH-REGULATING FACTOR 6*, *CYTOCHROME P450 90B1*, *KINASE-INDUCIBLE DOMAIN INTERACTING 9*, *E2FE*, *MYB DOMAIN PROTEIN 104*, *RESPONSE REGULATOR 7*, *INDOLE-3-ACETIC ACID INDUCIBLE 19*, *SEEDSTICK* (**Table S4**) (Sauret-Güeto et al., 2013; Omidbakhshfard et al., 2015; Gómez-Ocampo et al., 2023; Gonzalez et al., 2015; Vlieghe et al., 2005; Dubos et al., 2010; Lee et al., 2008; Maki et al., 2022; Lopes et al., 2023). In particular, the gene set associated with petal area was significantly enriched in genes involved in the regulation of flower and shoot system development (six genes, the two top significant terms, P~0.01), and regulation of reproductive process and development (12 genes, P~0.02) (**Table S5**). Overall, we found little to no overlap between flower organ size and leaf size-associated SNPs, consistently with the lack of pairwise phenotypic and genetic correlations between these traits (**Fig. 1d**). A few genes were associated with both leaf and sepal growth, but were detected by organ specific SNPs, suggesting that the underlying mutations may affect the function of general growth regulators in an organ-specific manner. Despite notable phenotypic correlations, the genetic determinants of the size of the flower organs exhibited limited overlap, consistently with a lack of clear genetic correlations. We thus concluded that the size of different flower organs largely evolves independently. The significant phenotypic correlations observed are thus more likely to reflect covariation of genetically independent traits that similarly respond to environmental changes rather than shared genetic bases.

Flower-size genes are under a mixed selection pattern in Arabidopsis thaliana.

The reduction in flower organ size following the transition to self-fertilization is anticipated to result from the reallocation of resources no longer required for pollinator attraction to other traits, benefiting fitness. According to this theory, new mutations underlying a reduction in flower size should be selectively favoured and accumulate in selfing lineages. To assess this hypothesis, we computed the

total effect size and estimated the allele ancestry of the detected SNPs from all gene sets (see Methods). Our results show that over three-fourths of the SNPs' derived alleles had a positive effect on the petal area (**Fig. 2a**). After scaling the SNP effects, we performed an ANOVA among all traits and demonstrated that an excess of positive effect among derived alleles exists in petal area only (**Fig. 2b**).

To test whether the fixation of derived alleles increasing flower size could result from genetic drift, we first computed genome-wide πN/πS. This ratio compares the accumulation of putatively disruptive mutations (πN, non-synonymous diversity) with the accumulation of neutral mutations (πS, synonymous diversity), thereby providing insights into the direction and intensity of selective pressures. Interestingly, petal area genes' πN/πS distribution was skewed and tended to drop below the genome average (P-value < 0.1). This observation is not consistent with a relaxation of selective pressure acting on these genes but rather suggests that they remain under significant evolutionary constraints. (**Fig. 2c**). Other flower organ size traits did not appear similarly skewed but also did not show any increase compared to the genome-wide average (**Fig. S3**). Moreover, while a majority of *a priori* petal candidate genes were located below the genome-wide average, three candidates, *AT1G36940*, *KIX9* and *FLM*, show abnormally elevated values among the top 5% genome-wide estimates, suggesting that these genes may undergo diversifying selection in amino acid sequences.

Next, we formally tested whether derived alleles from petal area candidate genes undergo positive selection. At a bi-allelic site, individuals carrying the allele under positive selection should share a longer surrounding haplotype than individuals carrying the ancestral allele due to ongoing selective sweeps. We estimated the decay of particular haplotypes as a function of distance from a focal SNP by computing genome-wide extended haplotype homozygosity (EHH) (Klassmann & Gautier, 2022). Under positive selection, the ratio of both alleles' EHH, standardized by the allele frequency (the integrated haplotype homozygosity score, iHS) exceeds the genome-wide average. Two petal area SNPs had an allele associated with a significantly longer EHH. The first one had a positive effect on petal area, likely by affecting the growth regulation factors *JMJ18* (snp_1_10937139, P-value = 0.013). The second selected allele (snp_5_870273, P-value = 0.02) reduces petal area likely by affecting AT5G03480, a less studied RNA-binding protein expressed in early petal development. We noted that a third moderately significant SNP, having a large petal allele under positive selection, likely affecting the flowering regulator *FLM* (snp_1_28960616; P-value = 0.07) (**Fig. 2d**). As a control, we performed the same analysis for all flower and leaf traits. We then estimated the enrichment of SNPs associated with the different traits in the 0.05% tail of the genome-wide iHS distribution (Tsuchimatsu et al., 2020). We observed a 3-fold enrichment in leaf size-associated SNPs, while no enrichment for flower size-associated SNPs was detected (**Fig. S4**). We conclude that there is a lack of unidirectional selection on flower size genetic determinants in *A. thaliana*: neither purifying selection nor positive selection drives flower size consistently across populations. The observed variation may result from heterogeneous patterns of more local differentiation and neutral processes enhanced by the small effective size and

strong population structure of the species. We next tested the hypothesis that the observed flower size organs' phenotypic and genetic variation results from heterogeneous selective pressures across the species' distribution range.

The influence of flower size on individual's performance is environment dependent

The observation that alleles increasing flower size can be under positive selection in selfing species challenges resource allocation theory that predicts an increase in fitness associated with the decline of flower organ growth investments in species such as *A. thaliana*. We thus investigated the relationship between petal size variation and plant performance across populations and under contrasted experimental conditions. We used fitness data available from a common garden experiment repeated across three sites, Valencia, Spain; Norwich, United Kingdom and Halle, Germany; (Wilczek et al., 2014). To maximise the overlap between fitness and petal size data, and to remove the non-genetic partition of petal area variation, we predicted petal size data for the whole set of 1135 re-sequenced *A. thaliana* accessions using the coefficients of a Bayesian sparse linear model ((Zhou et al., 2013), see Methods) and compared predicted petal size with fitness estimates in each experiments. Consistently with the selfing syndrome expectations, genotypes carrying small petal alleles performed better than those carrying large petal alleles in most studied environments (**Fig 2e and Fig S5**). However, the relationship between fitness and petal area varied across environments. This relationship was generally best fitted by a quadratic model, peaking at relatively small petals in Norwich and Valencia and at intermediate petal sizes in Halle. However, under increased environmental constraints (e.g., in summer and autumn in Norwich), it shifted to a linear negative relationship, suggesting a trade-off between flower size and fitness in those conditions. Similarly, we observed a negative relationship between petal size and fitness in other datasets (Fig. S5), though this trend disappeared under highly stressful conditions. Overall, these results indicate that individual performance is influenced by the genetic predisposition to invest in petal growth. However, the strength and shape of this relationship depend on environmental conditions. Such environment dependency of the relationship between flower size and fitness could result in heterogeneous selection regimes shaping petal size variation across the species range.

Habitat suitability influences the selection regime at flower size loci.

Our analysis, so far, suggests that the fitness cost or advantage associated with investing in flower growth in *A. thaliana* is contingent upon local environmental conditions. To test this idea further, we computed the habitat suitability from the collecting sites of the studied *A. thaliana* populations. We used the *MaxEnt* software (Phillips et al., 2006) to generate a species distribution model based on climatic data (Karger et al., 2017), altitude data (Danielson & Gesch, 2011), and an extensive species occurrence dataset from (Yim et al., 2024). We extracted the habitat suitability of each studied population (**Fig. 3a, Fig. S6**) and their limiting factor (**Fig. S7**). We observed a significant positive

relationship between accessions' petal area and the habitat suitability of their collecting site (**Fig. 3b**). However, the relationship was not linear but rather triangular due to the heteroscedasticity of the residuals: petal area variance increases with increasing habitat suitability. This was demonstrated by quantile regression comparison, where the 0.05 quantile regression was significantly different from the 0.95 quantile regression. This pattern suggests that petal size evolution is highly constrained at the climatic edge of the distribution where environmental factors limit the species expansion (Yim et al., 2024), whereas less directional selection is observed in favourable habitats. While a similar pattern was reported with flowering time (Yim et al., 2024), we tested whether such a pattern is common in *A. thaliana* phenotypes by testing heteroscedasticity across different datasets (**Fig. 3c**). None of the 107 phenotypes from (Atwell et al., 2010) presented a significant triangular relationship with habitat suitability. Among the 16 phenotypes from (Przybylska et al., 2023), only whole plant dry mass had a significant positive and triangular relationship with habitat suitability. In our dataset, in addition to petal area, sepal length also had both a significant positive and triangular relationship with habitat suitability. Moreover, across datasets, several phenotypes responded to habitat suitability in a homoscedastic manner. A significant positive correlation was found for all sepal traits (our dataset), three flowering time estimates (Atwell et al., 2010) and flowering time and leaf dry mass-related traits (Pryzbylska et al., 2023). A negative relationship was found with leaf length (our dataset), rosette diameter and time to senescence (Atwell et al., 2010), fruit and inflorescence length, and leaf nitrogen content (Pryzbylska et al., 2023). Together, these observations suggest that plant growth and life cycle strategies align with the suitability of plant's habitat. In addition, several phenotypes including flower organ size undergo a variance reduction in particular in less suitable environments.

To investigate on the origin of this phenotypic pattern, we next studied how petal size alleles distribute and are selected along the habitat suitability gradient. Consistently with the overall petal size response to the environment, large petal alleles increase in frequency towards more suitable habitats (**Fig. 3d**). We tested whether this may result from the different levels of purifying selection acting on small flowers along the species' distribution range. Purifying selection prevents the spread of new mutations, which results in an excess of rare, derived alleles in the distribution of allele frequencies (high skewness). The intensity of purifying selection can thus be determined by assessing changes in the distribution of derived allele frequencies, which can be achieved by computing the unfolded site frequency spectrum (SFS). We observed that low-frequency alleles ($0.05 < \text{Freq.} < 0.1$) were equally abundant in petal and leaf-associated genes, about one-fourth of analysed SNPs (**Fig. 3e**). We then observed the change in SFS shape along the HS gradient. The petal genes' SFS had a significantly higher skewness at low suitability compared to high suitability habitats, indicating stronger purifying selection at the less suitable edge of the species' distribution. By contrast, no significant shape difference was observed among leaf genes' SFS distributions. The molecular evolution of genes regulating flower size appears, thus, more constrained in less favourable habitats and relaxed in more favourable habitats, consistently

with the observed phenotypic variation. This observation suggests that the accumulation of large petal alleles in populations thriving in suitable habitats mostly results from the relaxation of the fitness penalty incurred by large petals.

Habitat heterogeneity and complex selection pattern maintain flower size variation in A. thaliana

Contrary to expectations from resource allocation theory, our findings suggest that petal size variation in *A. thaliana* is not constrained by a consistent trade-off with fitness but instead responds to a combination of local evolutionary drivers. While the cost or disadvantage of producing large flowers, particularly in a species capable of generating up to a thousand flowers (Exposito-Alonso et al., 2018), has selectively maintained small flowers in less suitable habitats, this constraint appears to be relaxed in more favorable regions, providing opportunities for mutations that increase petal size to become established. The difference in selection pressures across environments may explain the greater variance in flower size observed in genotypes originating from more favorable habitats. A limitation of our study is that our design does not explicitly account for gene-by-environment (G × E) interactions, which are inherently difficult to assess across such a broad range of environmental conditions. As a result, our measured petal size may not fully reflect phenotypes under natural conditions, potentially affecting our ability to capture the true relationship between flower size, geography and fitness. However, while flower size varies with environmental conditions, the proportion of variance explained by G × E for this trait is relatively small, and the plastic responses primarily reflect variation in the magnitude of a similar directional response to environmental factors (Wiszniewski et al., 2022). Consequently, petal size rankings among genotypes are likely to remain largely conserved across most environmental conditions. Indeed, we observed a significant correlation between our prediction of petal area and measurements from other studies, such as flower diameter at 17 degrees ($R = 0.35$, P-value < 0.01), flower diameter at 23 degrees ($R = 0.46$, P-value < 0.01) (Wiszniewski et al., 2022). Furthermore, selective pressures acting on genes associated with flower size mirror the observed phenotypic trends, further indicating that functional constraints on small-flower alleles become stronger at the species' climatic edge.

In addition to a relaxation of purifying selection, we detected signatures of positive selection acting on derived large-petal alleles particularly in the species' most suitable habitats, indicating that an increase in petal size may be advantageous under certain circumstances or at least when environment does not constraint individual's performance. Thus, further studies are needed to understand the adaptive value of 'large' flower size alleles in *A. thaliana*. This might be associated with the persistence of a low but significant probability of cross-fertilization in the species (Abbott & Gomes, 1989; Hoffmann et al., 2003), that may have been selected during post-glacial expansions northward, following secondary contact in the Iberian Peninsula (Fulgione & Hancock, 2018). Until today, the natural variation of selfing rate (s) across a large sample of *A. thaliana* populations have been reported once (Platt et al., 2010). We detected a positive correlation between the outcrossing rate (log(1-s)) and petal area (R =

0.25, P-value = 0.12) and Petal length (R = 0.32, P-value = 0.05) (**Fig. S8**). The lack of overlapping genotypes (N=39) and the lack of strong statistical significance prevent from drawing a conclusion about the role of petal area in outcrossing in *A. thaliana* might inspire future studies. Other ecological factors may also promote larger flowers and should be explored in future studies, including historical interactions with floral enemies (Galen, 1999), protection against microbial and viral infections (Vannette, 2020), and the role of flower thermogenesis in pollen germination (van der Kooi et al., 2019). Pleiotropy and linked selection could also contribute to the emergence of large-flower alleles, especially since some variants associated with petal size occur within genes known to affect other phenotypes or organs (Hanemian et al., 2020). Although genetic correlations suggest a limited contribution of these factors, further functional studies will be needed to identify the causal mutations and rigorously evaluate their developmental consequences and fitness benefits.

This study reveals significant variation in the investment in reproductive organs, particularly flower size, across the habitat range of *A. thaliana*. Theoretical predictions based on a pervasive evolutionary trend in the plant kingdom, the shift from outcrossing to selfing, propose that, in selfing lineages, flower size is predominantly negatively correlated with fitness, promoting the fixation of small flower alleles. Our findings support this proposition, but only in situations where environmental suitability declines, likely limiting the plants' capacity to acquire resources. In more favourable environments, the relaxation of purifying selection imposes fewer constraints on investment in flower growth, thus facilitating the evolution of large flower variants. This study highlights how changes in habitat suitability, influencing life history strategies, can initiate local trade-offs that alter the trajectory of phenotypic evolution.

Methods

Biological materials

For this study, we subsampled 407 *Arabidopsis thaliana* accessions from (Przybylska et al. 2023 data), originally selected for their extensive geographic and genetic coverage (**Fig. S1, Table S1**). All accessions were vernalized for 4 weeks in the dark at 5°C in October 2022. Seedlings were then transferred to soil in individual pots and grown in a glasshouse in semi-controlled conditions in Montpellier, CEFE CNRS, France (maintained around 20°C day and 15°C night with natural light). Accessions were randomly distributed on three tables daily rotated to homogenize the effect of spatial heterogeneity within the glasshouse across the genotypes. We used a single replicate per accession which allowed to maximize the genetic diversity coverage in a restricted experimental area, while genetic relatedness between accessions provided partial genetic replicates. Variance analysis within and between *Arabidopsis thaliana* regional populations (Alonso-Blanco et al., 2016) revealed high heritability for all investigated traits (**Table S2**), indicating strong phenotypic similarity among groups. Plants were surveyed daily, and the date of first flower opening, flower collection and plant death were recorded. Three flowers were collected between the 10th and the 25th flower of the main stem from the

primary inflorescence. Flowers were collected and preserved in 70% ethanol in individual Eppendorf placed in the dark at room temperature.

Morphological measurements

Flowers were stained with 0.02% Toluidine Blue for 10 minutes before been dissected and placed in between microscope slides and cover slips with a drop of glycerol (40% v/v). Slides were scanned at a 4800-dpi resolution with an Epson perfection v850 pro® scanner. Leaf, petal, sepal, and short and long stamen sizes (length, width, and area when relevant) were measured using Fiji version 2.35 (Schindelin et al., 2012). The blue channel of the images was isolated, and contrast-enhanced with Otsu's local contrast method. Pixels that belong to the organs were counted to estimate organ sizes. Measures were calibrated using the dots per inch (dpi) of the images. The ovule number per flower was counted manually using fluorescence microscopy (Leica DMI4000). Flowering time was calculated as the duration in days from seed sowing to the opening of the first flower. To estimate the genotype leaf sizes, while limiting environmental effects, the fourth leaf of every individual was collected at maturity and immediately scanned at 800dpi resolution. We computed an unbiased predictor of each trait by extracting the residuals of a linear model containing the relevant confounding factors (petal rank along the stem, stem number and a variable describing the spatial distribution in the tables). All traits were normally distributed and did not necessitate transformation (**Fig. S2**). We used our phenotypes in conjunction with published datasets that shared a significant number of accessions. In particular, we used the 107 phenotypes gathered by (Atwell et al., 2010), containing phenology, microbial resistance, plant morphology and ions content values, and the *Aradiv* database from (Przybylska et al., 2023) that contains plant functional strategies related traits. We also used datasets reporting fitness in terms of seed production where a majority of our accession set was shared, such as in (Exposito-Alonso et al., 2018; Wilczek et al., 2014), and compared our measurement of flower organ size with other available datasets (Li et al., 2020; Wiszniewski et al., 2022).

Statistical analyses

All statistical analyses were performed with R (version 4.3.2). We performed principal component analyses with *FactoMineR*. Testing for isometry versus allometry was achieved with standard major axis regression, which assumes an error component from both tested variables, with the package *smatr* (Warton et al., 2006). Skewness and deviation from the average were statistically tested in R using a skewness test and a Student's t-test, respectively.

Genome-Wide Association Study (GWAS)

We performed GWAS by testing the association between the above measured organ sizes with publicly available variant calling format (VCF) data from the 1001 genomes project webpage (https://1001genomes.org/data/GMI-MPI/releases/v3.1/) (Alonso-Blanco et al., 2016). Although single

replicate per accession may reduce detection power by introducing environmental noise, the high heritability of the measured traits and population structure signals associated with phenotypic variation suggest that increasing replicates per accession would have minimal impact on genetic association power (Kang et al., 2008). Moreover, our measurement of petal size correlated significantly with independent flower diameter measurements, i.e. the ranking from small to large flower genotypes remains consistent in between treatments (Wiszniewski et al., 2022) and across experiments (Spearman's Rank Correlation Coefficient ~ 0.46). Only single nucleotide polymorphisms (SNPs) were kept in the analyses, short indels and non-ACTGN were filtered out, as well as SNPs with a minor allele frequency below 5% using PLINK (Purcell et al. 2007). A total of 1,899,962 SNPs passed the filters. GWAS were performed using the GEMMA software v0.98.1 (Zhou & Stephens, 2012), which considers the population structure in a relatedness matrix. The proportion of phenotypic variance explained by the genotypes (PVE, the SNP-based heritability) was estimated for each trait with the *bslmm* function (Bayesian sparse linear mixed model). The P-values distribution of all GWAS followed a uniform distribution and did not necessitate transformation for false discovery rate. Specific quantitative trait loci (QTL) associated with the traits were located in two ways. First, we sought major QTL by a genome-wide screening of the association significance, accounting for multiple testing with Bonferroni corrected significance threshold. Second, to consider the potential polygenic architecture of the studied traits, we relaxed the threshold of significance. As there is no consensus on a threshold to detect multiple minor effect variants in a polygenic architecture (also known as multiple disease phenotype), reports of P-values detecting relevant genes range from 10-7 to 10-4 (Burton et al., 2007; Chen et al., 2021), we used an empirical approach and set the threshold at a P-value where we detected the FLOWERING LOCUS C (FLC) among the flowering time GWAS association peaks (P-value of 5.2*10-5). FLC, known as a key regulator of flowering time, is commonly detected in GWAS in A. thaliana, and its variation accounts for more than half the trait's variation (Sasaki et al., 2018). To eliminate genetically linked variants, we filtered out significant SNPs by considering their genomic position (https://www.arabidopsis.org), statistical significance, and predicted function using SnpEff (Cingolani MMB, 2012). This process resulted in retaining one focal polymorphism per QTL for subsequent analyses (Table S4). SNP effect sizes were estimated from the bslmm outputs, as recommended by Zhou et al. (2013) by the formula $\alpha + \beta.\gamma$, with α the small additive effect of each SNP, β the additional effect of some large effect SNPs and γ its posterior inclusion probability estimate. Estimation of the coefficients were further used to predict traits values for all 1,135 sequenced genotypes of the 1001 genome project using the predict function from GEMMA (Karasov et al., 2024; Lo et al., 2024).

Population Genetics Analysis

We assessed the regime of selection acting on leaf and flower size QTLs across the species distribution with two metrics. We first computed the $\pi N/\pi S$ ratio for all *A. thaliana* annotated genes. We calculated

the ratio between the genes' nucleotide diversity in non-synonymous sites (πN – defined as the 0-fold degenerate sites) and the nucleotide diversity in synonymous sites (πS – defined as 4-fold degenerate sites). The rationale is that πS gives a measure of neutral genetic variation and serve as a reference for πN which measures the amount of genetic variation at sites under natural selection control. Thus, a value of πN/πS below 1 is indicative of purifying selection, and a value above 1 is indicative of diverging selection. We used the genome-wide distribution as a reference: individual genes' πN/πS included in the 0.05 to 0.95 quantile do not deviate from the general purifying trend, Student test and skew test were performed on R to evaluate a set of genes πN/πS deviation from average and normality. Full sequences of gene coding regions and general feature format files were downloaded from Phytozome 13 (version Athaliana_447_TAIR10). Together with the VCF file, they were used to generate the diversity of gene sequences observed among *A. thaliana* genotypes. The R package *RGenetics* was used to discriminate 4-fold from 0-fold degenerate sites, and the *nuc.div* function from *pegas* was used to compute the nucleotide diversity. More details about the methods and scripts used are available at (https://github.com/kevinfrsartori/Whole_Genome_PiNPiS). Second, the extended haplotype homozygosity (EHH) was computed genome-wide to test whether a particular derived variant is subjected to ongoing or partial sweep in populations (Sabeti et al., 2002). When advantageous mutations are selected, the frequency of genetically linked variants also increases, extending the haplotype length around the selected site. This signal perdures until recombination events erase it. EHH measure the decay of a haplotype length upstream and downstream of the focal SNP, which thus depends on the selection's history and strength. Since the patterns of EHH might also be affected by the species' population structure and demographic history (Voight et al., 2006), we compute this estimate genome-wide to assess significance. The R package *rehh* (Gautier and Vitalis Bioinformatics, 2012) was used to compute the EHH's test statistic (iHS), defined as the log ratio of the integral of the EHH decay (iHH) around the derived allele divided by the iHH around the ancestral allele. This statistic was then compared to the distribution of iHS for all SNPs of similar allele frequency, and a P-value was reported. The iHS computation relies on the polarization of the SNP dataset, i.e. the ancestral state of each SNP. To differentiate between the derived versus ancestral allele, we used a maximum likelihood method using the focal species allele frequencies together with related species allelic information. We first identified an ortholog gene in *Arabidopsis lyrata* and *Arabidopsis halleri* for most *Arabidopsis thaliana* genes by using OrthoFinder (Emms & Kelly, 2015). We kept all *A. thaliana* genes having at least one ortholog and kept only one ortholog per outgroup species based on the genes' distance tree, resulting in a list of 25411 genes. We extracted a sequence covering the coding region plus the cis- and trans-regulatory regions for all trio of genes, and performed a multiple alignment using MAFFT (Katoh et al., 2002). We extracted the allelic information of the outgroup species with custom R scripts and ran the program est-sfs (Keightley & Jackson, 2018). It is important to note that the computation of iHS was limited to the presence of ortholog genes, resulting in filtering out few SNP per trait lists (**Table S4**).

Habitat suitability

The *A. thaliana* niche was modelled using the MaxEnt software (Phillips et al., 2006) by reproducing the method from (Yim et al., 2024). Climatic data were downloaded from CHELSA v2.1 (https://chelsa-climate.org) at a resolution of 30 arc seconds (Karger et al., 2017). The species distribution modelling was performed with the following variable panel: the isothermality (ratio of diurnal variation to annual variation in temperatures, °C), the mean of daily minimum air temperature of the coldest month (°C), the annual range of air temperature (°C), mean daily mean air temperatures of the wettest quarter (°C), mean daily mean air temperatures of the warmest quarter (°C), precipitation seasonality (standard deviation of the monthly precipitation estimates, kg m-2), mean monthly precipitation amount of the wettest quarter (kg m-2 month-1), and mean monthly precipitation amount of the driest quarter (kg m-2 month-1). Altitude data at a resolution of 30 arc seconds come from the Global Multi-resolution Terrain Elevation Data 2010 (GMTED2010) (Danielson and Gesch 2011) and were downloaded from the USGS website. We used the extensive species occurrence data (N=672) provided by (Yim et al., 2024), which covers the distribution of the species in an evenly spaced manner (one sample per km2) to account for sampling bias. From the MaxEnt model, we estimated the habitat suitability (HS) and the limiting factor (LF) of all *A. thaliana* accessions' collecting sites (**Fig. S6 S7**). The HS metric scales from zero to one, while LF refers to the climatic variable that has the most significant impact on HS when changed while maintaining all others variable constant.. The relationships between traits and HS were tested using linear regressions. The apparent heteroscedasticity of several trait-HS relationships was tested by comparing the 0.95 and 0.05 quantile regressions (Peng, 2017) using the R package *quantreg*. Linear regressions were plotted when significant, and quantile regressions were plotted when the test for slope difference (Anova) was significant. All statistical analyses were performed with R (R Core Team, 2020). In order to test for selection regime shift along habitat suitability, we divided the *A. thaliana* accession set into ten equally sized sub-populations. To avoid the influence of over-sampling in some regions of the species distribution, we first pruned the accession list based on genetic relatedness. We used the PLINK software to estimate the number of accessions passing a filtering threshold of genetic relatedness ranging from r=0.1 to r tends to 1. We found that the number of related accessions stops dropping after 0.95 and remains constant while r tends to 1 (**Fig. S9**). We thus excluded 87 highly correlated accessions. HS ranges were obtained by dividing the HS distribution of unrelated accessions into ten quantiles, where each quantile contains about 100 accessions.

Selection regime along habitat suitability

The HS ranges obtained by splitting the A. thaliana accession into 10 populations by habitat suitability did not have a geographic and historic meaning for the species, which prevents from computing most classical population genetic metrics. We tested for changes in selection pressure by relying on allele frequency only. We used the sequencing dataset presented above and reduced the minimum allele

frequency threshold to a minimum allele count of 1. Only the SNPs having ancestry information located in the gene body were kept, and we computed the unfolded site frequency spectrum for leaf and flower organs associated genes by reporting the allele counts for ranges of allele frequency of 0.05.

Acknowledgments

We thank the Sicard, and Rosa groups for discussions and comments on the article. We thank Alexander Platt for valuable discussions and method sharing. The computation and data handling were provided by the Swedish National Infrastructure for Computing (SNIC) at Uppmax, partially funded by the Swedish Research Council through grant agreement no 2018-05973. This work was supported by the Swedish Research Council (grant 2018-04214) and the Novo Nordisk Foundation (NNF22OC0079830) to AS, JRL was supported by NIH award R35GM138300 and MJH was partially funded by the European Union (views and opinions expressed are however those of the author(s) only and do not necessarily reflect those of the European Union or the European Education and Culture Executive Agency (EACEA). Neither the European Union nor EACEA can be held responsible for them).

Author contributions

Conceptualization: KS, FV, CV and AS; investigations: KS, CFM, MJH, EG, PM and AE; Data analyses: KS and CFM; Materials and analysis tools contributions: DV and JRL; writing original draft KS and AS; writing –review & editing– All authors.

Declaration of interests

The authors declare no competing interests.

Main figure legends

Figure 1: Extensive flower size variation in *A. thaliana* results from low pleiotropic mutations.

a) A Principal component analysis (PCA) was performed on flower organs and leaf size excluding flowering time that was correlated post hoc and represented as a supplementary variable. Bar plots show trait correlations with principal components (PC), with colours indicating different organs as shown on the top right scheme: dark green, leaf; light green, sepal; white, petal; blue, stamen; pink, ovules. The biplot displays accession coordinates along the first two principal components (PC), with organ silhouettes representing extreme organ size values at the same scale; **b)** Pairwise relationships between organ sizes. Coefficients were obtained from standard major axis linear regressions. The top right plot illustrates the slope test for organ isometry (null hypothesis: slope = 1). **c)** Manhattan plots displaying the genomic regions surrounding the three significant associations peaks (based on Bonferroni threshold) detected for all studied traits. Dot colours indicate associations with the size of different

organs as depicted in a), while shapes correspond to the parameter analyzed (triangles indicate association with area, circles with width or short, and squares with length or long). The Red dashed line represents the Bonferroni threshold, while the blue dashed line represents the polygenic threshold. Blue rectangles materialize the annotated gene code numbers (following "ATxG" in TAIR nomenclature, with *x* being the chromosome number). **d)** Venn diagrams illustrating the lack of overlap between SNPs, genes and candidate genes associated with leaf and flower organs' size variation.

Figure 2: A variable flower size–seed production trade-off explains a mixed selection pattern on flower size in *A. thaliana*.

a) Distribution of derived alleles' total effect size from each peak of association identified in GWAS for petal area. Each square represents a SNP's derived allele, white and grey indicating a positive and negative effect, respectively. **b)** Distribution of derived alleles' total effect size from each peak of association identified in GWAS for each trait investigated. A p-value is given for trait distributions significantly different from 0 (vertical line). **c)** $\pi N/\pi S$ distribution across all *Arabidopsis thaliana* genes, among the petal area genes and a priori candidate genes identified in the GWAS for petal area. The dashed line represents the whole genome average. **d)** Extended haplotype homozygosity around FLM lead SNP position. The red and blue integrals represent the degree of haplotype identity shared by individuals carrying the C (derived) and T (ancestral) alleles, respectively, as a function of distance to the lead SNP (dashed line). **e)** Relationship between the genetic variance of petal area and seed production across different experimental fields; hau, Halle autumn; vau, Valencia autumn; nsp, Norwich spring; nsu, Norwich summer; nau, and Norwich autumn. Triangles represent the modelled petal size that maximizes seed production, black lines represent the best fit (anova) between a linear and a quadratic regressions, and blue shadows represent the confidence intervals of the regressions.

Figure 3: Habitat suitability shapes patterns of phenotype diversification across the geographical range of *A. thaliana*.

a) Map of the studied European accessions. The orange to purple scale represents the modelled habitat suitability from less to more suitable, and the blue dots represent accessions' collecting sites. **b)** Correlation between petal area and habitat suitability. Lines represent significant regressions: plain line, linear model; dashed lines, 0.05 and 0.95 quantile regressions. **c)** Large petal alleles' frequency along habitat suitability clusters. **d)** Unfolded site frequency spectrum (SFS) among SNPs located in petal and leaf gene sets. The colours of the bars correspond to the habitat suitability classes. Inserts represent the relationship between the SFS's shape and habitat suitability, where a plain line depicts significant and dashed line insignificant correlation.

References

Adler, M. I., Cassidy, E. J., Fricke, C., & Bonduriansky, R. (2013). The lifespan-reproduction trade-off under dietary restriction is sex-specific and context-dependent. *Experimental Gerontology*, *48*(6), 539–548. https://doi.org/10.1016/j.exger.2013.03.007

Alonso-Blanco, C., Andrade, J., Becker, C., Bemm, F., Bergelson, J., Borgwardt, K. M., Cao, J., Chae, E., Dezwaan, T. M., Ding, W., Ecker, J. R., Exposito-Alonso, M., Farlow, A., Fitz, J., Gan, X., Grimm, D. G., Hancock, A. M., Henz, S. R., Holm, S., … Zhou, X. (2016). 1,135 Genomes Reveal the Global Pattern of Polymorphism in Arabidopsis thaliana. *Cell*, *166*(2), 481–491. https://doi.org/10.1016/j.cell.2016.05.063

Atwell, S., Huang, Y. S., Vilhjálmsson, B. J., Willems, G., Horton, M., Li, Y., Meng, D., Platt, A., Tarone, A. M., Hu, T. T., Jiang, R., Muliyati, N. W., Zhang, X., Amer, M. A., Baxter, I., Brachi, B., Chory, J., Dean, C., Debieu, M., … Nordborg, M. (2010). Genome-wide association study of 107 phenotypes in Arabidopsis thaliana inbred lines. *Nature*, *465*(7298), 627–631. https://doi.org/10.1038/nature08800

Barrett, S. C. H., Arunkumar, R., & Wright, S. I. (2014). The demography and population genomics of evolutionary transitions to self-fertilization in plants. *Philosophical Transactions of the Royal Society B: Biological Sciences*, *369*(1648), 20130344. https://doi.org/10.1098/rstb.2013.0344

Burton, P. R., Clayton, D. G., Cardon, L. R., Craddock, N., Deloukas, P., Duncanson, A., Kwiatkowski, D. P., McCarthy, M. I., Ouwehand, W. H., Samani, N. J., Todd, J. A., Donnelly, P., Barrett, J. C., Burton, P. R., Davison, D., Donnelly, P., Easton, D., Evans, D., Leung, H.-T., … Primary Investigators. (2007). Genome-wide association study of 14,000 cases of seven common diseases and 3,000 shared controls. *Nature*, *447*(7145), Article 7145. https://doi.org/10.1038/nature05911

Buysse, S. F., Pérez, S. G., Puzey, J. R., Garrison, A., Bradburd, G. S., Oakley, C. G., Tonsor, S. J., Picó, F. X., Josephs, E. B., & Conner, J. K. (2024). *Evaluating the Roles of Drift and Selection in Trait Loss along an Elevational Gradient* (p. 2024.06.12.598645). bioRxiv. https://doi.org/10.1101/2024.06.12.598645

Caruso, C. M. (2006). Adaptive evolution: The ecological genetics of floral traits. *Heredity*, *97*(2), 86–87. https://doi.org/10.1038/sj.hdy.6800853

Charlesworth, D., & Charlesworth, B. (1981). Allocation of resources to male and female functions in hermaphrodites. *Biological Journal of the Linnean Society*, *15*(1), 57–74. https://doi.org/10.1111/j.1095-8312.1981.tb00748.x

Chebib, J., & Guillaume, F. (2017). What affects the predictability of evolutionary constraints using a G-matrix? The relative effects of modular pleiotropy and mutational correlation. *Evolution*, *71*(10), 2298–2312. https://doi.org/10.1111/evo.13320

Chen, Z., Boehnke, M., Wen, X., & Mukherjee, B. (2021). Revisiting the genome-wide significance threshold for common variant GWAS. *G3 Genes|Genomes|Genetics*, *11*(2), jkaa056. https://doi.org/10.1093/g3journal/jkaa056

Crane, P. R., Friis, E. M., & Pedersen, K. R. (1994). Palaeobotanical evidence on the early radiation of magnoliid angiosperms. In P. K. Endress & E. M. Friis (Eds.), *Early Evolution of Flowers* (pp. 51–72). Springer. https://doi.org/10.1007/978-3-7091-6910-0_4

Danielson, J. J., & Gesch, D. B. (2011). *Global Multi-resolution Terrain Elevation Data 2010 (GMTED2010): U.S. Geo- logical Survey Open-File Report 2011* (p. 26). https://www.researchgate.net/publication/264159030_Global_Multi-resolution_Terrain_Elevation_Data_2010_GMTED2010

Dubos, C., Stracke, R., Grotewold, E., Weisshaar, B., Martin, C., & Lepiniec, L. (2010). MYB transcription factors in Arabidopsis. *Trends in Plant Science*, *15*(10), 573–581. https://doi.org/10.1016/j.tplants.2010.06.005

Emms, D. M., & Kelly, S. (2015). OrthoFinder: Solving fundamental biases in whole genome comparisons dramatically improves orthogroup inference accuracy. *Genome Biology*, *16*(1), 157. https://doi.org/10.1186/s13059-015-0721-2

Exposito-Alonso, M., Vasseur, F., Ding, W., Wang, G., Burbano, H. A., & Weigel, D. (2018). Genomic basis and evolutionary potential for extreme drought adaptation in Arabidopsis thaliana. *Nature Ecology & Evolution*, *2*(2), 352–358. https://doi.org/10.1038/s41559-017-0423-0

Friis, E. M., Pedersen, K., & Crane, P. (2006). Cretaceous angiosperm flowers: Innovation and evolution in plant reproduction. *Palaeogeography, Palaeoclimatology, Palaeoecology*, *232*, 251–293. https://doi.org/10.1016/j.palaeo.2005.07.006

Friis, E. M., Pedersen, K. R., & Crane, P. R. (1994). Angiosperm floral structures from the Early Cretaceous of Portugal. In P. K. Endress & E. M. Friis (Eds.), *Early Evolution of Flowers* (pp. 31–49). Springer. https://doi.org/10.1007/978-3-7091-6910-0_3

Friis, E. M., Pedersen, K. R., & Crane, P. R. (1999). Early Angiosperm Diversification: The Diversity of Pollen Associated with Angiosperm Reproductive Structures in Early Cretaceous Floras from Portugal. *Annals of the Missouri Botanical Garden*, *86*(2), 259. https://doi.org/10.2307/2666179

Fu, L., Wang, S., Liu, Z., Nijs, I., Ma, K., & Li, Z. (2010). Effects of resource availability on the trade-off between seed and vegetative reproduction. *Journal of Plant Ecology*, *3*(4), 251–258. https://doi.org/10.1093/jpe/rtq017

Galen, C. (1999). Why Do Flowers Vary?The functional ecology of variation in flower size and form within natural plant populations. *BioScience*, *49*(8), 631–640. https://doi.org/10.2307/1313439

Gómez-Ocampo, G., Crocco, C. D., Cascales, J., Oklestkova, J., Tarkowská, D., Strnad, M., Mora-Garcia, S., Pruneda-Paz, J. L., Blazquez, M. A., & Botto, J. F. (2023). BBX21 Integrates Brassinosteroid Biosynthesis and Signaling in the Inhibition of Hypocotyl Growth under Shade. *Plant and Cell Physiology*, pcad126. https://doi.org/10.1093/pcp/pcad126

Gonzalez, N., Pauwels, L., Baekelandt, A., De Milde, L., Van Leene, J., Besbrugge, N., Heyndrickx, K. S., Cuéllar Pérez, A., Durand, A. N., De Clercq, R., Van De Slijke, E., Vanden Bossche, R., Eeckhout, D., Gevaert, K., Vandepoele, K., De Jaeger, G., Goossens, A., & Inzé, D. (2015). A Repressor Protein Complex Regulates Leaf Growth in Arabidopsis. *The Plant Cell*, *27*(8), 2273–2287. https://doi.org/10.1105/tpc.15.00006

Hanemian, M., Vasseur, F., Marchadier, E., Gilbault, E., Bresson, J., Gy, I., Violle, C., & Loudet, O. (2020). Natural variation at FLM splicing has pleiotropic effects modulating ecological strategies in Arabidopsis thaliana. *Nature Communications*, *11*(1), 4140. https://doi.org/10.1038/s41467-020-17896-w

Hoffmann, M. H., Bremer, M., Schneider, K., Burger, F., Stolle, E., & Moritz, G. (2003). Flower Visitors in a Natural Population of Arabidopsis thaliana. *Plant Biology*, *5*(5), 491–494. https://doi.org/10.1055/s-2003-44784

Huala, E., Dickerman, A. W., Garcia-Hernandez, M., Weems, D., Reiser, L., LaFond, F., Hanley, D., Kiphart, D., Zhuang, M., Huang, W., Mueller, L. A., Bhattacharyya, D., Bhaya, D., Sobral, B. W., Beavis, W., Meinke, D. W., Town, C. D., Somerville, C., & Rhee, S. Y. (2001). The Arabidopsis Information Resource (TAIR): A comprehensive database and web-based information retrieval, analysis, and visualization system for a model plant. *Nucleic Acids Research*, *29*(1), 102–105. https://doi.org/10.1093/nar/29.1.102

Huxley, J. S., Churchill, F. B., & Strauss, R. E. (1993). *Problems of Relative Growth*. Johns Hopkins University Press. https://doi.org/10.56021/9780801846595

Johnson, K., & Lenhard, M. (2011). Genetic control of plant organ growth. *New Phytologist*, *191*(2), 319–333. https://doi.org/10.1111/j.1469-8137.2011.03737.x

Kang, H. M., Zaitlen, N. A., Wade, C. M., Kirby, A., Heckerman, D., Daly, M. J., & Eskin, E. (2008). Efficient Control of Population Structure in Model Organism Association Mapping. *Genetics*, *178*(3), 1709–1723. https://doi.org/10.1534/genetics.107.080101

Karasov, T. L., Neumann, M., Leventhal, L., Symeonidi, E., Shirsekar, G., Hawks, A., Monroe, G., Exposito-Alonso, M., Bergelson, J., Weigel, D., & Schwab, R. (2024). Continental-scale associations of Arabidopsis thaliana phyllosphere members with host genotype and drought. *Nature Microbiology*, *9*(10), 2748–2758. https://doi.org/10.1038/s41564-024-01773-z

Karger, D. N., Conrad, O., Böhner, J., Kawohl, T., Kreft, H., Soria-Auza, R. W., Zimmermann, N. E., Linder, H. P., & Kessler, M. (2017). Climatologies at high resolution for the earth's land surface areas. *Scientific Data*, *4*, 170122. https://doi.org/10.1038/sdata.2017.122

Katoh, K., Misawa, K., Kuma, K., & Miyata, T. (2002). MAFFT: A novel method for rapid multiple sequence alignment based on fast Fourier transform. *Nucleic Acids Research*, *30*(14), 3059. https://doi.org/10.1093/nar/gkf436

Keightley, P. D., & Jackson, B. C. (2018). Inferring the Probability of the Derived vs. The Ancestral Allelic State at a Polymorphic Site. *Genetics*, *209*(3), 897–906. https://doi.org/10.1534/genetics.118.301120

Klassmann, A., & Gautier, M. (2022). Detecting selection using extended haplotype homozygosity (EHH)-based statistics in unphased or unpolarized data. *PLoS ONE*, *17*(1). https://doi.org/10.1371/JOURNAL.PONE.0262024

Kozłowski, J. (1992). Optimal allocation of resources to growth and reproduction: Implications for age and size at maturity. *Trends in Ecology & Evolution*, *7*(1), 15–19. https://doi.org/10.1016/0169-5347(92)90192-E

Lee, D. J., Kim, S., Ha, Y.-M., & Kim, J. (2008). Phosphorylation of Arabidopsis response regulator 7 (ARR7) at the putative phospho-accepting site is required for ARR7 to act as a negative regulator of cytokinin signaling. *Planta*, *227*(3), 577–587. https://doi.org/10.1007/s00425-007-0640-x

Li, X., Zhang, Y., Yang, S., Wu, C., Shao, Q., & Feng, X. (2020). The genetic control of leaf and petal allometric variations in Arabidopsis thaliana. *BMC Plant Biology*, *20*(1), 1–11. https://doi.org/10.1186/s12870-020-02758-w

Lo, C.-Y., Chien, C.-C., Lin, Y.-P., Yeh, P.-M., & Lee, C.-R. (2024). *How weedy Arabidopsis thaliana dominated the world: Ancestral variation and polygenic adaptation* (p. 2024.04.28.591542). bioRxiv. https://doi.org/10.1101/2024.04.28.591542

Lopes, A. L., Moreira, D., Pereira, A. M., Ferraz, R., Mendes, S., Pereira, L. G., Colombo, L., & Coimbra, S. (2023). AGPs as molecular determinants of reproductive development. *Annals of Botany*, *131*(5), 827–838. https://doi.org/10.1093/aob/mcad046

MacTavish, R., & Anderson, J. T. (2020). Resource availability alters fitness trade-offs: Implications for evolution in stressful environments. *American Journal of Botany*, *107*(2), 308–318. https://doi.org/10.1002/ajb2.1417

Maki, Y., Soejima, H., Sugiyama, T., Watahiki, M. K., Sato, T., & Yamaguchi, J. (2022). 3-Phenyllactic acid is converted to phenylacetic acid and induces auxin-responsive root growth in Arabidopsis plants. *Plant Biotechnology*, *39*(2), 111–117. https://doi.org/10.5511/plantbiotechnology.21.1216a

Omidbakhshfard, M. A., Proost, S., Fujikura, U., & Mueller-Roeber, B. (2015). Growth-Regulating Factors (GRFs): A Small Transcription Factor Family with Important Functions in Plant Biology. *Molecular Plant*, *8*(7), 998–1010. https://doi.org/10.1016/j.molp.2015.01.013

Parker, G. A., & Smith, J. M. (1990). Optimality theory in evolutionary biology. *Nature*, *348*(6296), Article 6296. https://doi.org/10.1038/348027a0

Peng, R. K., Victor Chernozhukov, Xuming He, Limin (Ed.). (2017). *Handbook of Quantile Regression*. Chapman and Hall/CRC. https://doi.org/10.1201/9781315120256

Pérez-Harguindeguy, N., Díaz, S., Garnier, E., Lavorel, S., Poorter, H., Jaureguiberry, P., Bret-Harte, M. S., Cornwell, W. K., Craine, J. M., Gurvich, D. E., Urcelay, C., Veneklaas, E. J., Reich, P. B., Poorter, L., Wright, I. J., Ray, P., Enrico, L., Pausas, J. G., de Vos, A. C., … Cornelissen, J. H. C. (2013). New handbook for standardised measurement of plant functional traits worldwide. *Australian Journal of Botany*, *61*(3), 167. https://doi.org/10.1071/BT12225

Phillips, S. J., Anderson, R. P., & Schapire, R. E. (2006). Maximum entropy modeling of species geographic distributions. *Ecological Modelling*, *190*(3), 231–259. https://doi.org/10.1016/j.ecolmodel.2005.03.026

Platt, A., Horton, M., Huang, Y. S., Li, Y., Anastasio, A. E., Mulyati, N. W., Ågren, J., Bossdorf, O., Byers, D., Donohue, K., Dunning, M., Holub, E. B., Hudson, A., Le Corre, V., Loudet, O., Roux, F., Warthmann, N., Weigel, D., Rivero, L., … Borevitz, J. O. (2010). The Scale of Population Structure in Arabidopsis thaliana. *PLoS Genetics*, *6*(2), e1000843. https://doi.org/10.1371/journal.pgen.1000843

Poecke, R. M. P. V. (2007). Arabidopsis-Insect Interactions. *The Arabidopsis Book*, *2007*(5). https://doi.org/10.1199/tab.0107

Przybylska, M. S., Violle, C., Vile, D., Scheepens, J. F., Lacombe, B., Le Roux, X., Perrier, L., Sales-Mabily, L., Laumond, M., Vinyeta, M., Moulin, P., Beurier, G., Rouan, L., Cornet, D., & Vasseur, F.

(2023). AraDiv: A dataset of functional traits and leaf hyperspectral reflectance of Arabidopsis thaliana. *Scientific Data*, *10*(1), Article 1. https://doi.org/10.1038/s41597-023-02189-w

Roddy, A. B., Martínez-Perez, C., Teixido, A. L., Cornelissen, T. G., Olson, M. E., Oliveira, R. S., & Silveira, F. A. O. (2020). Towards the flower economics spectrum. *New Phytologist*, *n/a*(n/a). https://doi.org/10.1111/nph.16823

Sasaki, E., Frommlet, F., & Nordborg, M. (2018). GWAS with Heterogeneous Data: Estimating the Fraction of Phenotypic Variation Mediated by Gene Expression Data. *G3 Genes|Genomes|Genetics*, *8*(9), 3059–3068. https://doi.org/10.1534/g3.118.200571

Sauret-Güeto, S., Schiessl, K., Bangham, A., Sablowski, R., & Coen, E. (2013). JAGGED Controls Arabidopsis Petal Growth and Shape by Interacting with a Divergent Polarity Field. *PLoS Biology*, *11*(4), e1001550. https://doi.org/10.1371/journal.pbio.1001550

Sicard, A., & Lenhard, M. (2011). The selfing syndrome: A model for studying the genetic and evolutionary basis of morphological adaptation in plants. *Annals of Botany*, *107*(9), 1433–1443. https://doi.org/10.1093/aob/mcr023

Sicard, A., Stacey, N., Hermann, K., Dessoly, J., Neuffer, B., Bäurle, I., & Lenhard, M. (2011). Genetics, evolution, and adaptive significance of the selfing syndrome in the genus Capsella. *The Plant Cell*, *23*(9), 3156–3171. https://doi.org/10.1105/tpc.111.088237

Slotte, T. (2014). The impact of linked selection on plant genomic variation. *Briefings in Functional Genomics*, *13*(4), 268–275. https://doi.org/10.1093/bfgp/elu009

Smith, J. M., & Haigh, J. (1974). The hitch-hiking effect of a favourable gene. *Genetics Research*, *23*(1), 23–35. https://doi.org/10.1017/S0016672300014634

Stebbins, G. L. (1957). Self Fertilization and Population Variability in the Higher Plants. *The American Naturalist*, *91*(861), 337–354. https://doi.org/10.1086/281999

Stephan, W. (2019). Selective Sweeps. *Genetics*, *211*(1), 5–13. https://doi.org/10.1534/genetics.118.301319

Tsuchimatsu, T., Kakui, H., Yamazaki, M., Marona, C., Tsutsui, H., Hedhly, A., Meng, D., Sato, Y., Städler, T., Grossniklaus, U., Kanaoka, M. M., Lenhard, M., Nordborg, M., & Shimizu, K. K. (2020). Adaptive reduction of male gamete number in the selfing plant Arabidopsis thaliana. *Nature Communications 2020 11:1*, *11*(1), 1–9. https://doi.org/10.1038/s41467-020-16679-7

Tuller, J., Marquis, R. J., Andrade, S. M. M., Monteiro, A. B., & Faria, L. D. B. (2018). Trade-offs between growth, reproduction and defense in response to resource availability manipulations. *PLOS ONE*, *13*(8), e0201873. https://doi.org/10.1371/journal.pone.0201873

Vlieghe, K., Boudolf, V., Beemster, G. T. S., Maes, S., Magyar, Z., Atanassova, A., Engler, J. de A., Groodt, R. D., Inzé, D., & Veylder, L. D. (2005). The DP-E2F-like Gene DEL1 Controls the Endocycle in Arabidopsis thaliana. *Current Biology*, *15*(1), 59–63. https://doi.org/10.1016/j.cub.2004.12.038

Warton, D. I., Wright, I. J., Falster, D. S., & Westoby, M. (2006). Bivariate line-fitting methods for allometry. *Biological Reviews*, *81*(02), 259. https://doi.org/10.1017/S1464793106007007

Wilczek, A. M., Cooper, M. D., Korves, T. M., & Schmitt, J. (2014). Lagging adaptation to warming climate in Arabidopsis thaliana. *Proceedings of the National Academy of Sciences*, *111*(22), 7906–7913. https://doi.org/10.1073/pnas.1406314111

Wiszniewski, A., Uberegui, E., Messer, M., Sultanova, G., Borghi, M., Duarte, G. T., Vicente, R., Sageman-Furnas, K., Fernie, A. R., Nikoloski, Z., & Laitinen, R. A. E. (2022). Temperature-mediated flower size plasticity in Arabidopsis. *iScience*, *25*(11), 105411. https://doi.org/10.1016/J.ISCI.2022.105411

Worley, A. C., & Barrett, S. C. H. (2000). Evolution of Floral Display in Eichhornia Paniculata (pontederiaceae): Direct and Correlated Responses to Selection on Flower Size and Number. *Evolution*, *54*(5), 1533–1545. https://doi.org/10.1111/j.0014-3820.2000.tb00699.x

Woźniak, N. J., Kappel, C., Marona, C., Altschmied, L., Neuffer, B., & Sicard, A. (2020). A Similar Genetic Architecture Underlies the Convergent Evolution of the Selfing Syndrome in *Capsella*. *The Plant Cell*, *32*(4), 935–949. https://doi.org/10.1105/tpc.19.00551

Woźniak, N. J., & Sicard, A. (2018). Evolvability of flower geometry: Convergence in pollinator-driven morphological evolution of flowers. *Seminars in Cell & Developmental Biology*, *79*, 3–15. https://doi.org/10.1016/j.semcdb.2017.09.028

Yim, C., Bellis, E. S., DeLeo, V. L., Gamba, D., Muscarella, R., & Lasky, J. R. (2024). Climate biogeography of Arabidopsis thaliana: Linking distribution models and individual variation. *Journal of Biogeography*, *51*(4), 560–574. https://doi.org/10.1111/jbi.14737

Zhou, X., Carbonetto, P., & Stephens, M. (2013). Polygenic modeling with bayesian sparse linear mixed models. *PLoS Genetics*, *9*(2), e1003264. https://doi.org/10.1371/journal.pgen.1003264

Zhou, X., & Stephens, M. (2014). Efficient multivariate linear mixed model algorithms for genome-wide association studies. *Nature Methods*, *11*(4), 407–409. https://doi.org/10.1038/nmeth.2848

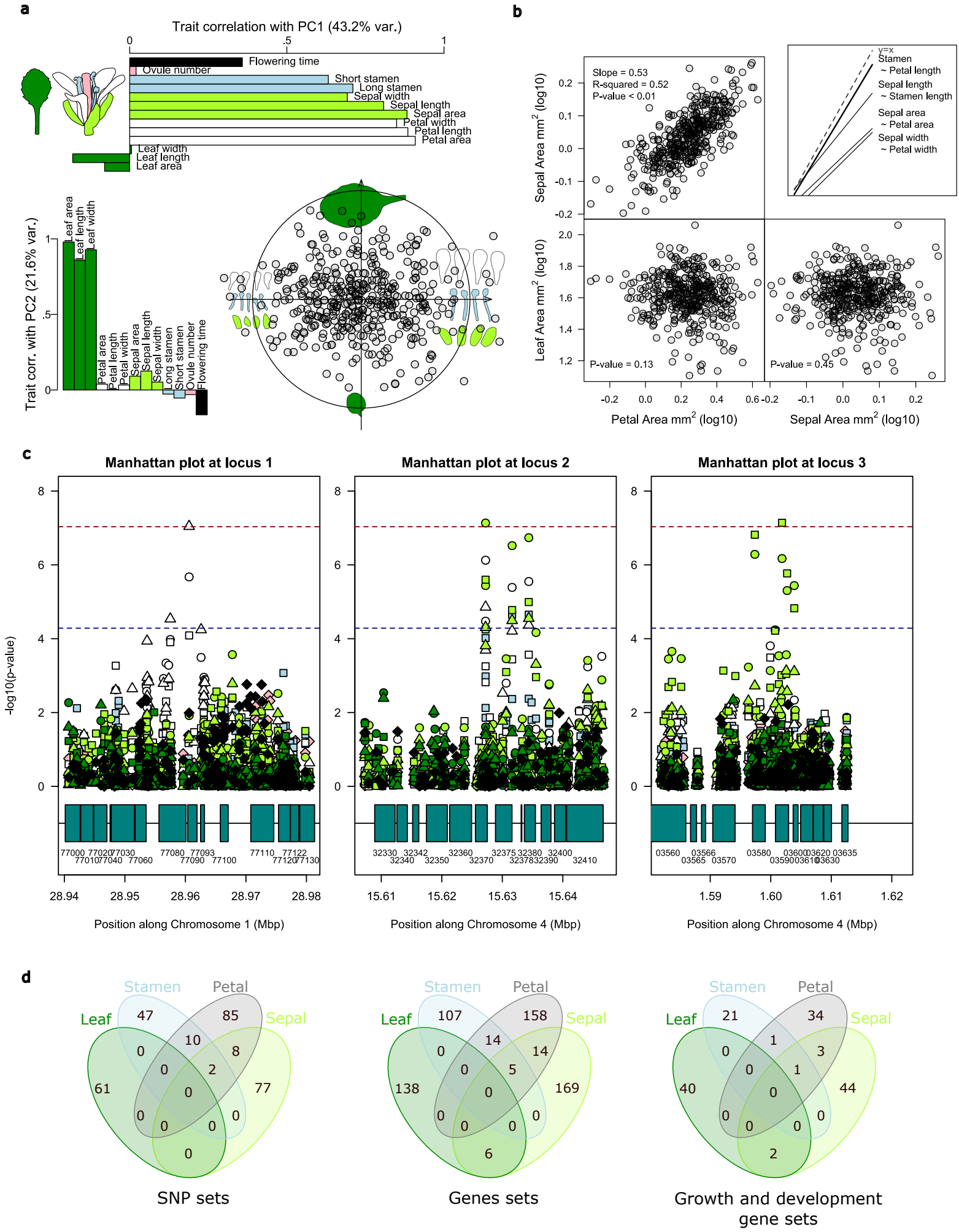
a
Trait correlation with PC1 (43.2% var.)
Flowering time
Ovule number
Short stamen
Long stamen
Sepal width
Sepal length
Sepal area
Petal width
Petal length
Petal area
Leaf width
Leaf length
Leaf area
Trait corr. with PC2 (21.6% var.)
b
Slope = 0.53
R-squared = 0.52
P-value < 0.01
y=x
Stamen ~ Petal length
Sepal length ~ Stamen length
Sepal area ~ Petal area
Sepal width ~ Petal width
Sepal Area mm2 (log10)
Leaf Area mm2 (log10)
P-value = 0.13
P-value = 0.45
Petal Area mm2 (log10)
Sepal Area mm2 (log10)
c
Manhattan plot at locus 1
Manhattan plot at locus 2
Manhattan plot at locus 3
-log10(p-value)
Position along Chromosome 1 (Mbp)
Position along Chromosome 4 (Mbp)
Position along Chromosome 4 (Mbp)
d
Stamen
Petal
Leaf
Sepal
SNP sets
Genes sets
Growth and development gene sets

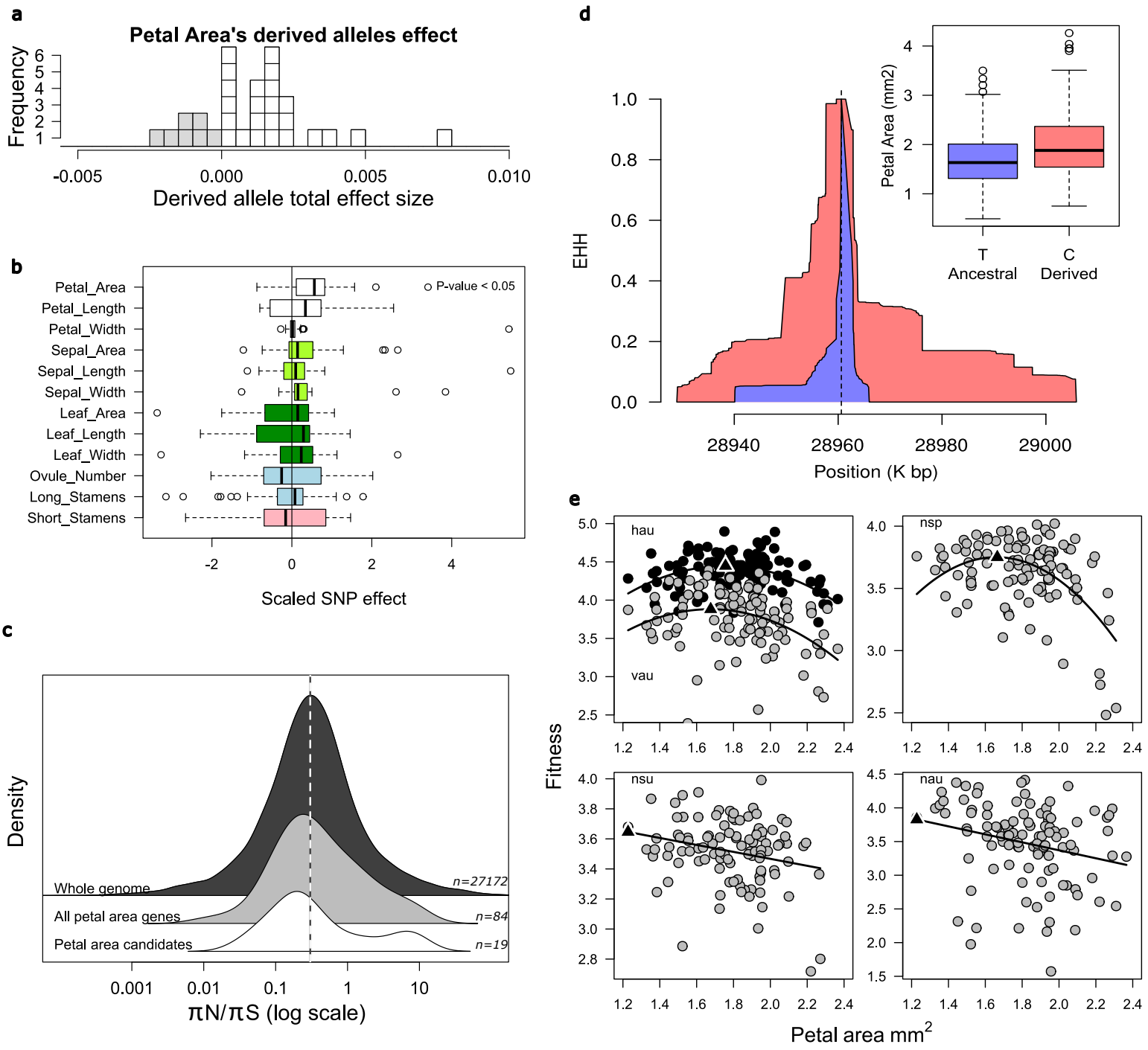
a
Petal Area's derived alleles effect
Frequency
Derived allele total effect size
b
P-value < 0.05
Petal_Area
Petal_Length
Petal_Width
Sepal_Area
Sepal_Length
Sepal_Width
Leaf_Area
Leaf_Length
Leaf_Width
Ovule_Number
Long_Stamens
Short_Stamens
Scaled SNP effect
c
Density
Whole genome
All petal area genes
Petal area candidates
n=27172
n=84
n=19
πN/πS (log scale)
d
EHH
Petal Area (mm2)
T
Ancestral
C
Derived
Position (K bp)
e
hau
vau
nsp
nsu
nau
Fitness
Petal area mm2

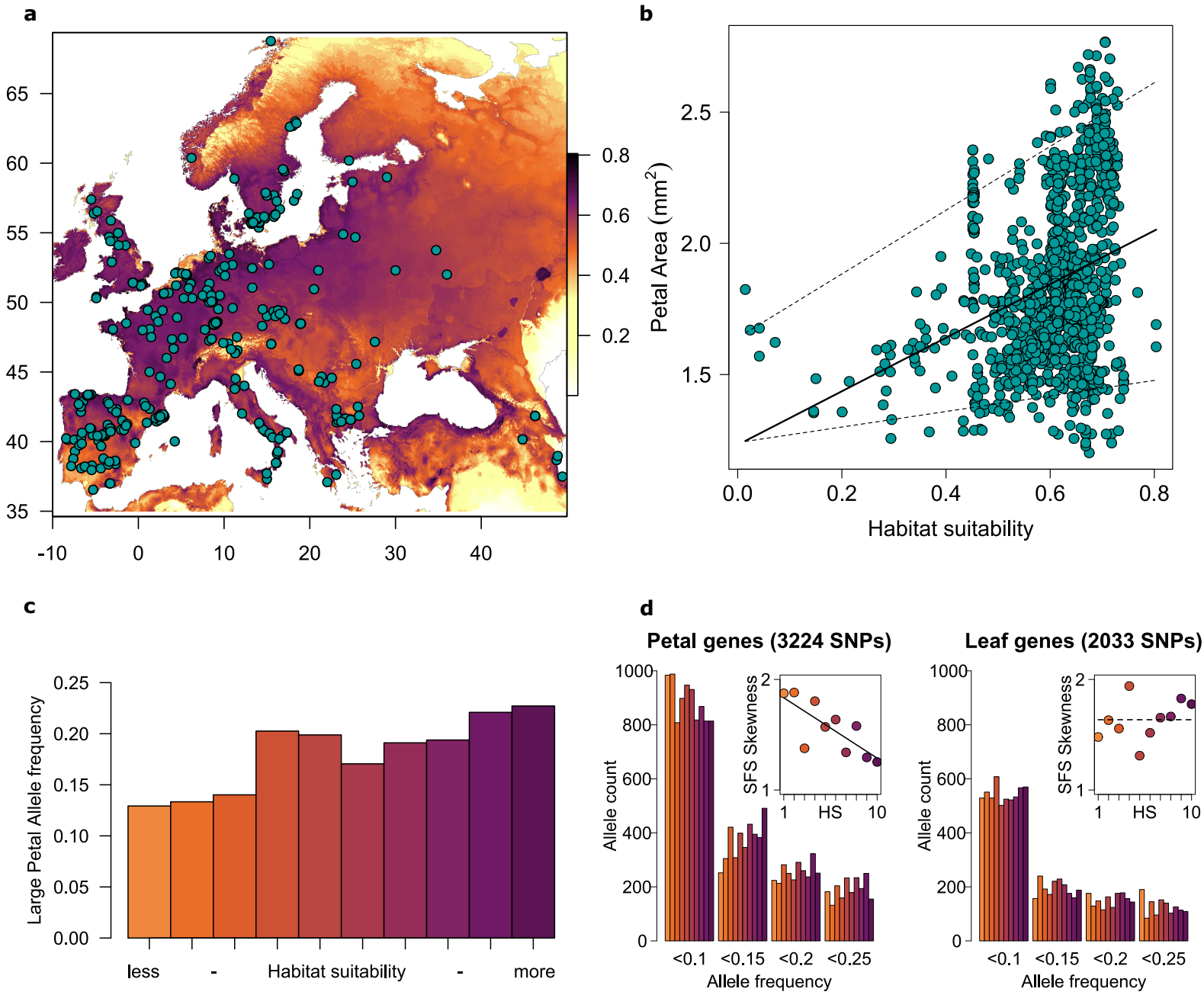

Figure 3: Habitat suitability shapes patterns of phenotype diversification across the geographical range of *A. thaliana*.
a) Map of the studied European accessions. The orange to purple scale represents the modelled habitat suitability from less to more suitable, and the blue dots represent accessions' collecting sites. b) Correlation between petal area and habitat suitability. Lines represent significant regressions: plain line, linear model; dashed lines, 0.05 and 0.95 quantile regressions. c) Large petal alleles' frequency along habitat suitability clusters. d) Unfolded site frequency spectrum (SFS) among SNPs located in petal and leaf gene sets. The colours of the bars correspond to the habitat suitability classes. Inserts represent the relationship between the SFS's shape and habitat suitability, where a plain line depicts significant and dashed line insignificant correlation.

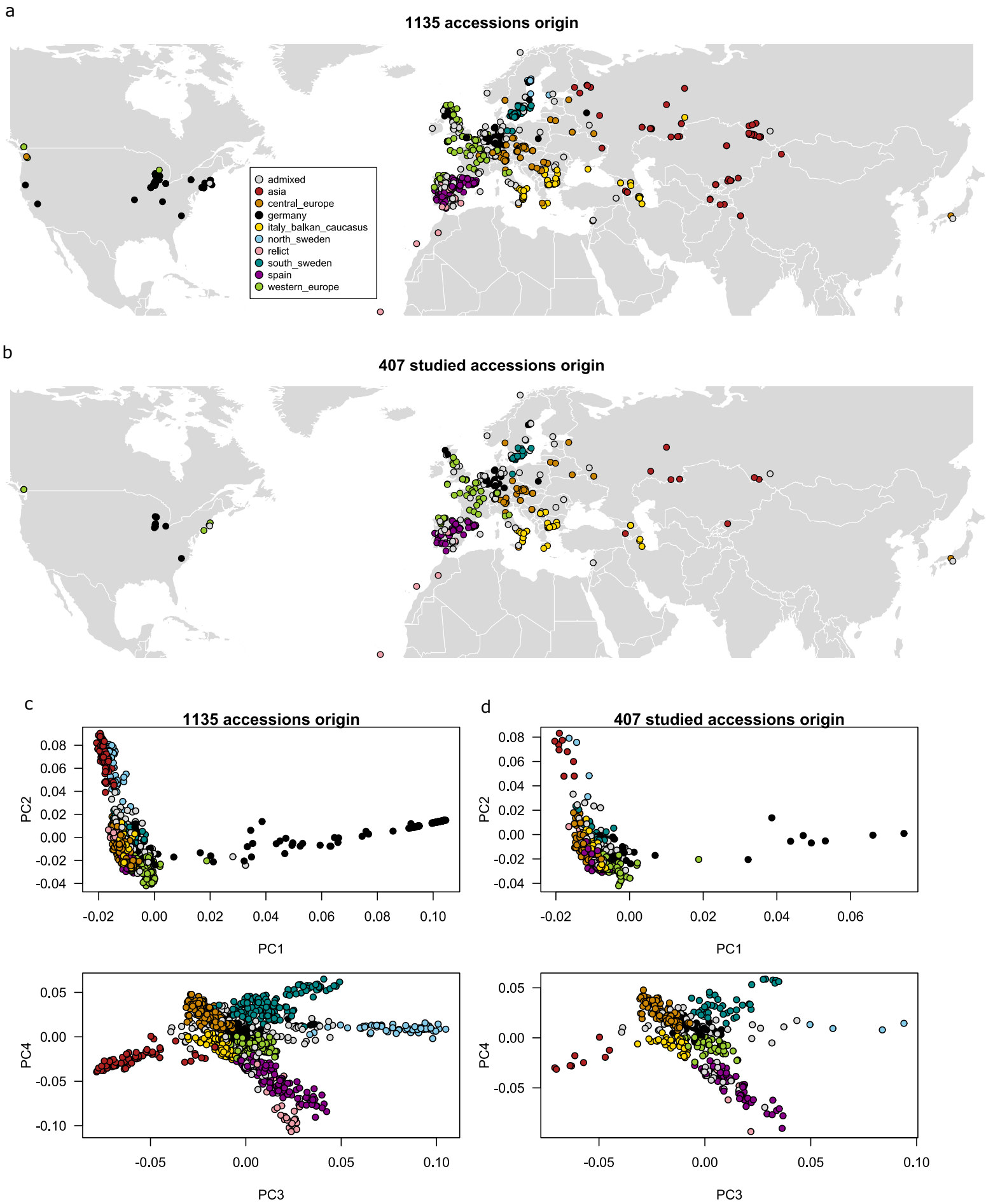

Figure S1 Geographic distribution and genetic differentiation of Arabidopsis thaliana accessions. A) Geographic distribution of all sequenced accessions from the 1001 genome project (N=1135). B) Distribution of the herein studied accessions (N = 407). C) and D) Distribution of the accessions on the four principal components of their genetic variation. Colors refer to the admixture analysis performed in the original paper from the 1001 genome project, and are reported on the above maps.

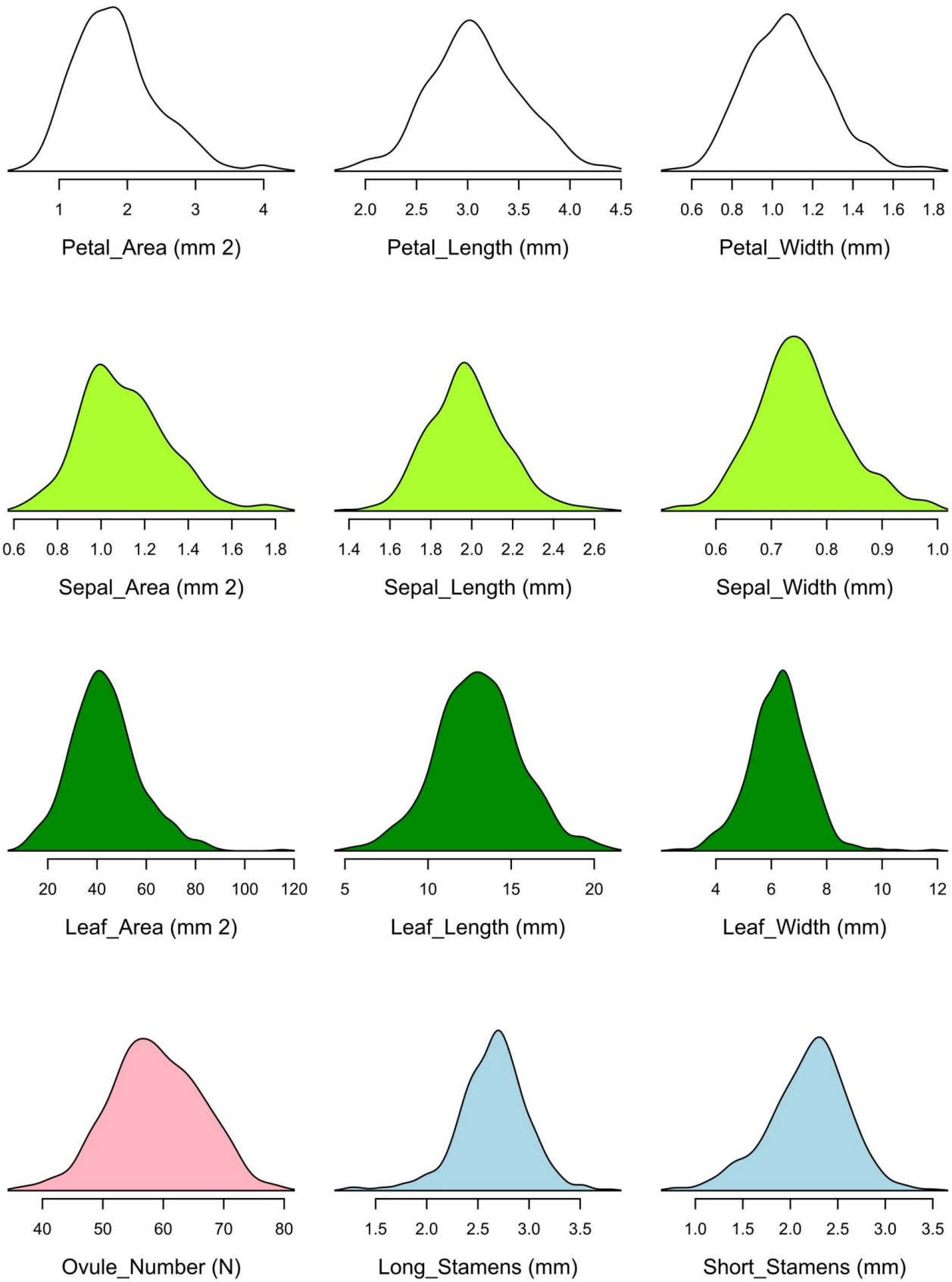

Figure S2. Distribution of the traits measured for this study. Colors represent only the color code used along the manuscript.

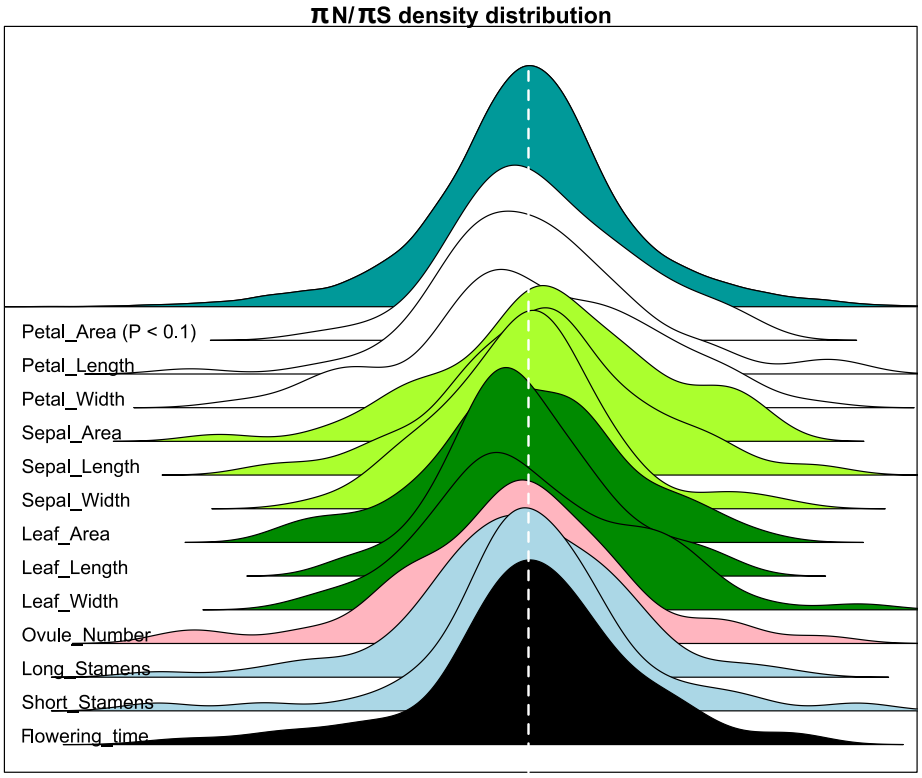

Figure S3. πN/πS distribution from genes associated with leaf and flower organ size traits, and flowering time. The dark blue distribution and its average (dashed white line) are from the genome wide computation. Traits names can be read at the left foot of the distributions. Pvalues indicate the significance of the mean difference between a trait and the genome wide distribution and are reported only if P<0.1.

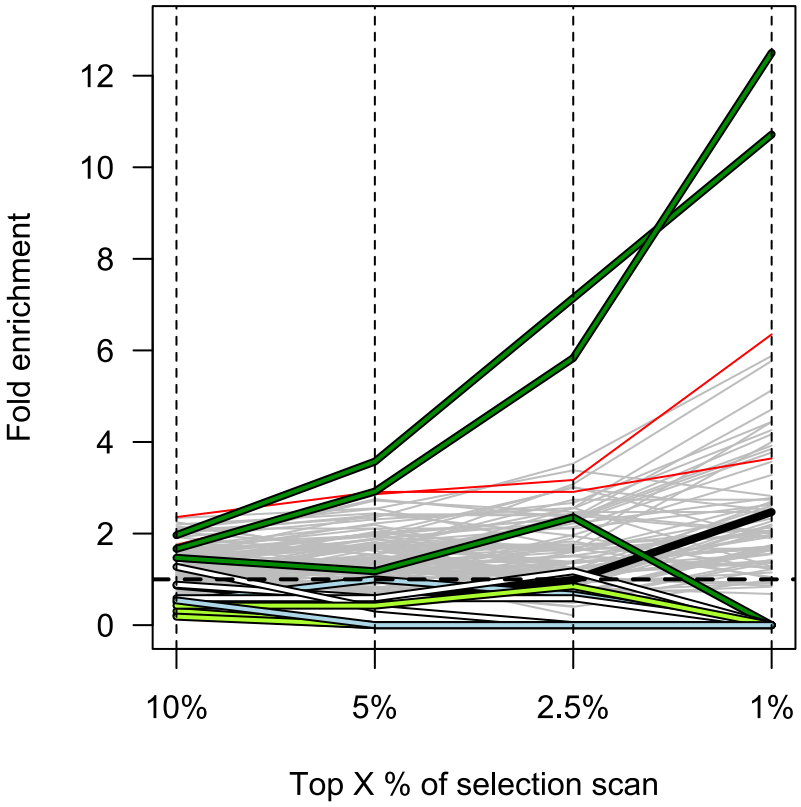

Figure S4. Fold enrichment of SNPs associated with a trait, among the most signicant SNPs on a genome wide scan for selection (Extended Haplotype Homozygosity). Color code can be seen in figure S3 above. Grey lines represent the fold enrichment of SNPs detected in GWAs for all 107 phenotypes from Atwell et al. 2010, red lines represent the enrichment detected for male and female gamete in Tsuchimatsu et al. 2020.

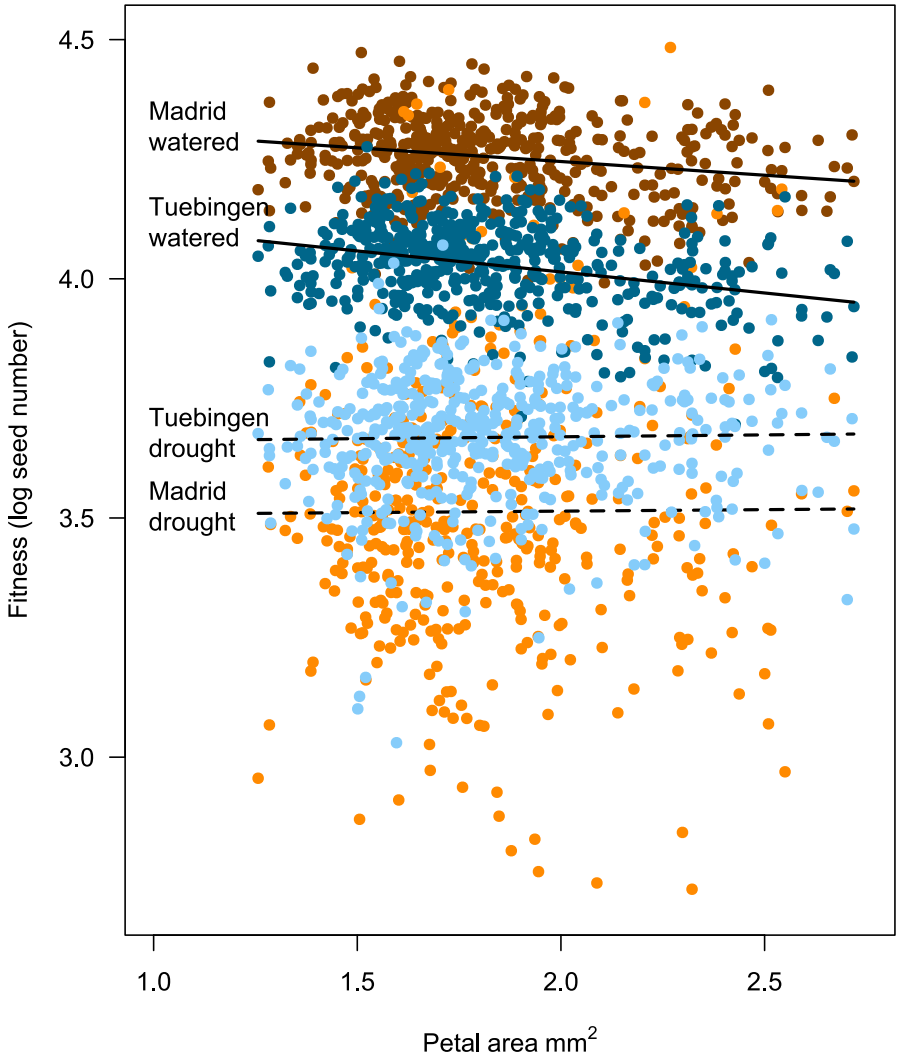

Figure S5. Fitness as a function of petal area across *Arabidopsis thaliana* accessions. Fitness data were recovered from (Exposito-Alonso et al. 2019). Petal area data were predicted from the coefficient of a Bayesian sparse linear mixed model to match the sampling of the fitness experiments. Bold lines represent significant linear regressions, dashed lines represent non significant regressions.

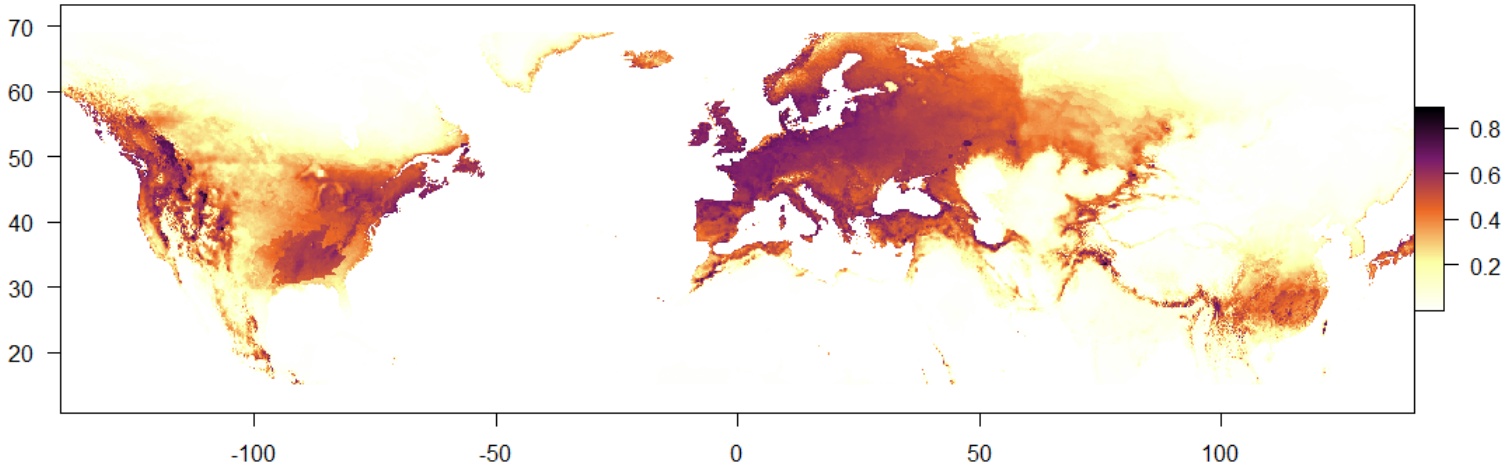

Figure S6. Predicted habitat suitability for *Arabidopsis thaliana* populations.

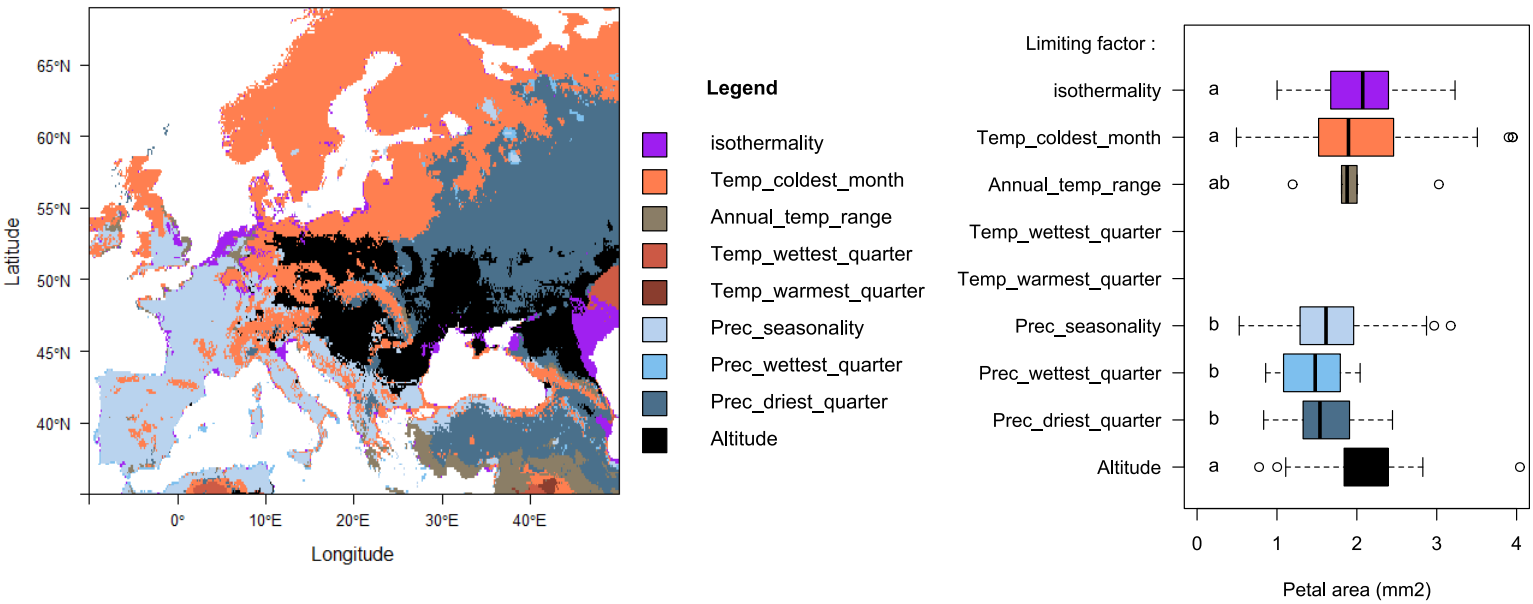

Figure S7. Distribution of the factors limiting the habitat suitability and their effect on petal area. a) Distribution of the limiting factors over Europe. b) Boxplots showing the distribution of petal area among accessions split by the limiting factor of their collecting site. Letters indicate significant differences determined by one-way ANOVA with Tukey's HSD test (α=0.05).

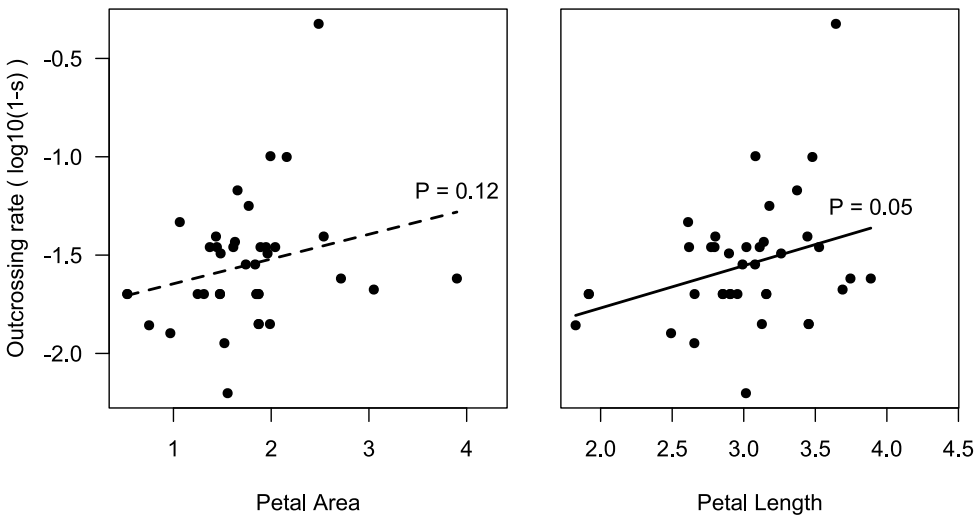

Figure S8. Outcrossing rate as a function of petal area and petal length. Each dot is a population of *Arabidopsis thaliana*, straight lines represent significant (bold) and unsignificant (dashed) relationships with associated Pvalues (P).

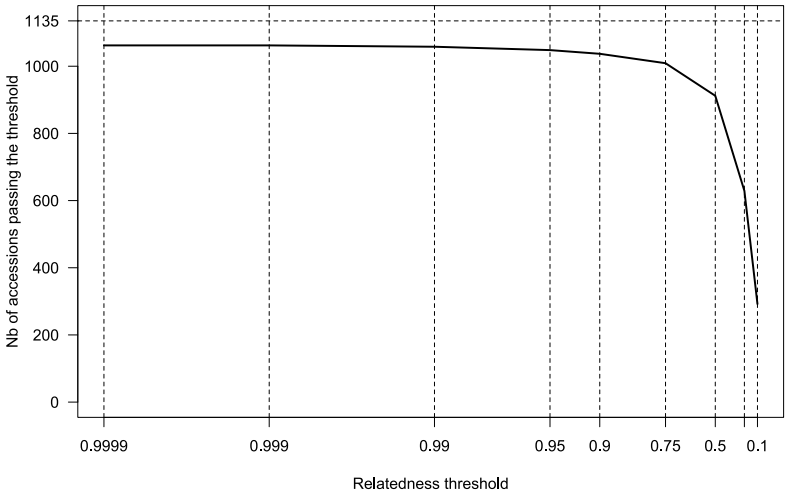

Figure S9. Genetic clones in the 1135 accesions set. A relatedness matrix computed on the SNP dataset was used to filter out "genetic clones" based on a threshold (x-axis) and the number of accessions passing the threshold was reported (y-axis)